RSC Chemical Biology

ROYAL SOCIETY OF CHEMISTRY

REVIEW

View Article Online
View Journal | View Issue

Cite this: *RSC Chem. Biol.*, 2025, 6, 338

Navigating the dichotomy of reactive oxygen, nitrogen, and sulfur species: detection strategies and therapeutic interventions

Prayasee Baruah, Dikshaa Padhi, Hariharan Moorthy, Madhu Ramesh and Thimmaiah Govindaraju *

Reactive oxygen, nitrogen and sulfur species (RONSS) collectively encompasses a variety of energetically dynamic entities that emerge as inherent characteristics of aerobic life. This broad category includes reactive oxygen species (ROS), reactive nitrogen species (RNS), and reactive sulfur species (RSS). A conundrum arises from the indispensable role of RONSS in redox signalling, while its overproduction in the mitochondria poses deleterious effects. This imbalance leads to biomolecular damage and contributes to neurodegenerative disorders, cancer, cardiovascular diseases and inflammation. Notably, the differential roles of RONSS across various diseases can be strategically exploited for therapeutic interventions. Timely, precise, and sensitive detection methods are indispensable for elucidating the spatiotemporal dynamics of RONSS and evaluating disease pathogenesis and progression. By monitoring RONSS levels, we can discern early markers of disease onset, enabling proactive intervention strategies for effective disease management. Therapeutic interventions targeting oxidative/nitrosative stress in disease pathologies have proven to be effective treatment routes in the mitigation of different diseases. This review aims to offer a comprehensive overview of the functional implications and delicate balance of RONSS in disease conditions, and advances made in detection strategies over the years while offering therapeutic strategies to tackle their adverse effects. A special emphasis is focussed on neurodegenerative disorders and cancer with case studies using RONSS-targeted chemical probes and prodrugs.

Received 15th January 2025,
Accepted 17th January 2025

DOI: 10.1039/d5cb00006h

rsc.li/rsc-chembio

Bioorganic Chemistry Laboratory, New Chemistry Unit, Jawaharlal Nehru Centre for Advanced Scientific Research, Jakkur P.O., Bengaluru, Karnataka 560064, India. E-mail: tgraju@jncasr.ac.in

1. Introduction

The paradoxical dependency of aerobic organisms on oxygen is an intriguing phenomenon because while essential for survival,

Prayasee Baruah

Prayasee Baruah received her BSc (Hons.) in Chemistry from Cotton College, Guwahati, Assam in 2014, and MSc in Chemistry from North-Eastern Hill University (NEHU), Shillong, Meghlaya in 2016. She obtained her PhD from NEHU in 2022 and is currently working as a post-doctoral researcher under the supervision of Prof. T. Govindaraju, JNCASR, Bengaluru. With a background in biophysical chemistry, her research interests include development of therapeutics for Alzheimer's Disease and ferroptosis via mitigation of different causative factors.

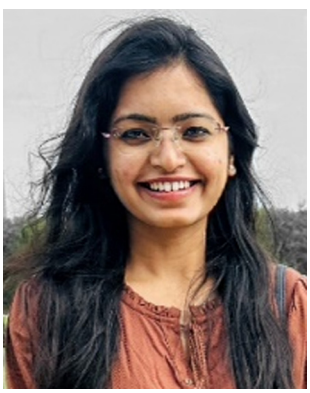

Dikshaa Padhi

Dikshaa Padhi received her Integrated BS-MS in Chemistry from Veer Surendra Sai University of Technology, Odisha, India, in 2018. In 2019, she joined for PhD at JNCASR, Bengaluru, under the mentorship of Prof. T. Govindaraju. Her research pursuits revolve around comprehending the diverse pathogenic mechanisms underlying Alzheimer's disease, investigating post-translational modifications, their role in phase separation, and the design of small molecules with therapeutic potential.

an excess of oxygen can have catastrophic consequences. This dichotomy of oxygen both nurtures and terminates life.[1,2] Reactive oxygen species (ROS) is a major class of reactive species that includes a variety of chemical compounds resulting from the partial reduction of oxygen.[3,4] In addition to ROS, RNS have also been extensively studied for their impact on redox homeostasis. In the 20th century, the field of redox biology primarily focused on metal ions, ROS, and RNS.[5–7] Collectively, RONSS exert a dichotomous influence on health and disease, playing pivotal yet contradictory roles. In addition, alkyl (R), alkoxy (RO), peroxyl (RO_2) radicals, and carbonyl oxides (R1R2COO) can engage in various unimolecular and bimolecular chemical processes. However, research on these is still in nascent stages and outside the scope of this review.

RONSS plays a pivotal role in maintaining optimal well-being through cellular signalling and transduction, protein phosphorylation, maintenance of ion channels, and biosynthesis of thyroid hormones (THs) by the thyroid gland. RONSS has also been utilized as part of therapeutic methods, especially in the annihilation of cancer cells. When oxidants exceed an organism's antioxidant defences, it can cause damage to cellular organelles (such as mitochondria) and biomolecules (like DNA, proteins, and lipids). This can lead to the onset of various disease conditions, including oxidative stress, inflammation, neurodegeneration, cancer, cardiovascular, liver, and kidney diseases (Fig. 1). Therefore, detection and neutralisation of RONSS are of significance in different pathological condtions.[8–12]

Detection strategies for RONSS are vital for identifying oxidative and nitrosative stress in disease contexts, enabling timely diagnosis and monitoring of disease progression. To effectively sense or treat RONSS in various diseases, achieving both sensitivity and specificity is essential. This requires strategies that target RONSS selectively while minimizing off-target effects. One approach is to design RONSS-specific molecules, such as fluorogenic/calorimetric probes, that activate fluorescence or colorimetric changes only in the presence of a specific RONSS type (*e.g.*, H_2O_2, HOCl, or $ONOO^-$). This selectivity relies on tailored chemical reactions that specifically recognize individual RONSS, thereby reducing cross-reactivity. Additionally, to enhance probe reliability, these molecules should be stable under physiological conditions, resistant to environmental factors such as pH variations, serum, and temperature, which can otherwise lead to non-specific signals.[13,14] For therapeutic applications, redox-active drugs can be designed to respond only to pathological RONSS levels, sparing normal cells. For instance, prodrugs activated by elevated concentrations of specific RONSS in cancer cells can provide selective cytotoxicity.[15] Nanotechnology further advances specificity by using targeted nanocarriers conjugated with antibodies or ligands that recognize disease-specific markers, allowing

Hariharan Moorthy

Hariharan Moorthy received his BSc in Chemistry (Hons) in 2017 and MSc in Chemistry in 2019 from Sri Sathya Sai Institute of Higher Learning (SSSIHL), Puttaparthi, Andhra Pradesh, India. He joined JNCASR in 2019 for the PhD programme under the supervision of Prof. T. Govindaraju. His research interest includes the development of multifunctional therapeutic macromolecules for targeting amyloid pathways, and ferroptosis which has implications in Alzheimer's disease.

Madhu Ramesh

Madhu Ramesh received his BVSc & AH in 2015 from Veterinary College, Bidar, Karnataka and MVSc in Biochemistry from Indian Veterinary Research Institute (IVRI), Bareilly, Uttar Pradesh, India. He obtained his PhD from JNCASR under the supervision of Prof. T. Govindaraju and is currently working as a postdoctoral researcher. His research interest includes understanding the pathophysiology to identify novel diagnostic and therapeutic targets and developing diagnostic and multifunctional therapeutic agents for Alzheimer's disease.

Thimmaiah Govindaraju

Thimmaiah Govindaraju is a Professor at the Bioorganic Chemistry Laboratory, New Chemistry Unit, JNCASR, Bengaluru, Karnataka, India. He received his MSc (2000) from Bangalore University and PhD in Chemistry (2006) from the National Chemical Laboratory and University of Pune, India. He carried out postdoctoral research at the University of Wisconsin-Madison, USA (2005–2006) and the Max Planck Institute of Molecular Physiology, Dortmund, Germany (2006–2008) as an Alexander von Humboldt postdoctoral fellow. His research interests are at the interface of chemistry, biology, and biomaterials science, including Alzheimer's disease, peptide chemistry, molecular probes, redox biology in disease pathogenesis, theranostics, molecular architectonics, and silk and cyclic dipeptide derived biomimetics.

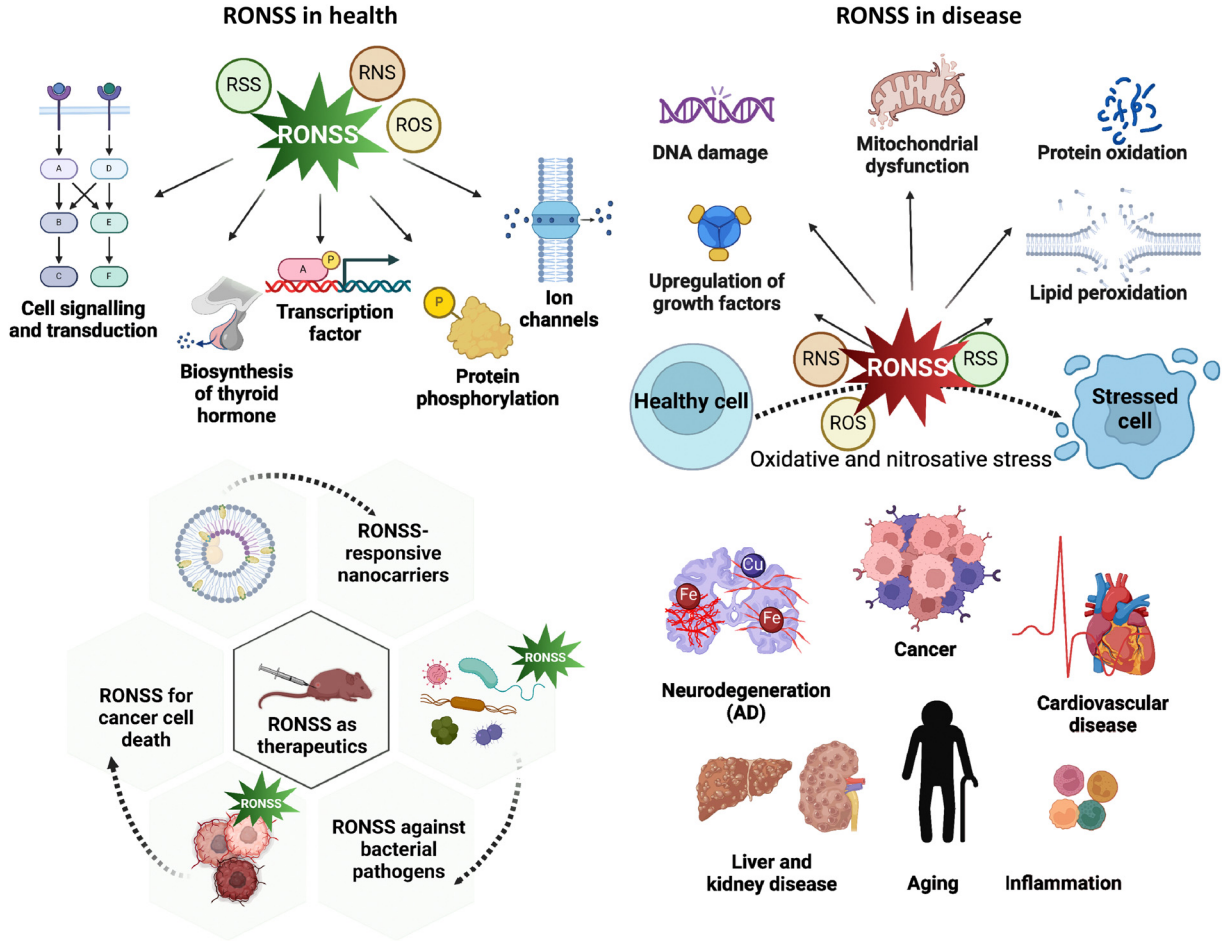

Fig. 1 Schematic shows the dichotomous role of RONSS in health and disease. RONSS: reactive oxygen, nitrogen and sulfur species, ROS: reactive oxygen species, RNS: reactive nitrogen species, and RSS: reactive sulfur species (created with https://www.biorender.com/).

precise delivery of RONSS-sensitive probes or therapeutic agents to affected tissues.[16] Additionally, enzyme-mimicking nanozymes designed to scavenge RONSS offer selective neutralization of RONSS in diseased tissues.[17] This approach combines diagnostic and therapeutic functions, providing potential for both monitoring and mitigating RONSS-related damage. These advancements enable more accurate, targeted approaches to detecting and treating RONSS-associated diseases.

2. The RONSS cycle: homeostasis

RONSS are generated endogenously as part of normal cellular physiology under pathological conditions or triggered by external environmental stressors such as air pollution, smoking, and pathogens. The mitochondrial respiratory chain is the primary source of cellular ROS, generated during ATP generation through normal oxygen metabolism.[18] Oxygen readily accepts electrons from cellular oxidative metabolism, generating ROS like superoxide anion ($O_2^{\bullet -}$), hydroxyl ($HO^{\bullet}$), and hydrogen peroxide (H_2O_2). Various processes like electron transport uncoupling and enzyme system activities (*e.g.*, cytochrome P450, xanthine oxidoreductase, inflammatory enzymes), and accumulation of unbound metal ions of Fe, Cu, and Mn can exacerbate ROS production.[19] NADPH Oxidase (NOX), certain membrane-bound proteins and the endoplasmic reticulum (ER) are also involved in the production of ROS. Nitric oxide (NO) is enzymatically produced by nitric oxide synthase (NOS) through a series of redox reactions. The biosynthesis of NO is the primary source of RNS production in biological systems through its rapid interaction with various ROS.[20] For example, NO with $O_2^{\bullet -}$ reacts at a diffusion-controlled rate to form the peroxynitrite anion ($ONOO^-$) and its conjugated acid, peroxynitrous acid (ONOOH). NO_2 is generated in an aqueous environment, through the isomerization of ONOOH.

The primary source of RSS is the mitochondrial sulfide oxidation pathway. At least four RSS are produced during the process of mitochondrial sulfide oxidation: persulfide, glutathione (GSH), thiosulfate, and sulfite. RSS are difficult to measure due to their high reactivity and instability.[21] However, over the past decade, there has been a renewed interest in the detection methods for H_2S and related RSS, largely attributed to the growing recognition of their pivotal and intricate roles in the maintenance of health.[22]

In the body, defence against oxidative stress or excess ROS involves the synergistic action of enzymatic and non-enzymatic antioxidants. The endogenous enzymatic antioxidants include superoxide dismutase (SOD), catalase (CAT), glutathione

peroxidase (GPX), and glutathione reductase (GR), which serve as the first line of defence against RONSS.[23] Non-enzymatic hydrophilic antioxidants include Nrf2-Keap 1 pathway, urate, ascorbate, GSH, and flavonoids, while lipophilic radical antioxidants comprise tocopherol, carotenoid, and ubiquinol. Glutathione *S*-transferases (GSTs), thioredoxin system, peroxiredoxins, and the paraoxonase family (PON1, PON2, PON3) detoxify xenobiotics and counteract cellular toxins.[24] Antioxidant formulations are also therapeutically used to combat oxidative stress associated with different disorders.

3. RONSS in healthy organism

There has been a growing appreciation of the role of ROS as mediators of intracellular signalling and regulation of numerous physiological and biological responses, such as growth factor signalling, cell division, differentiation, and adaptive responses necessary to maintain the living system.[25] ROS is known to interact with various proteins and regulate cell proliferation and apoptosis, *via* oxidation of redox-active residues such as tyrosine, histidine or cysteine, thus creating intra- or inter-protein bridges and modulating protein functions. The first-degree oxidation of cysteine residues catalysed by H_2O_2 within proteins serves as a reversible signal transduction mechanism in living cells.[26] ROS inhibit phosphatases, while simultaneously activating an extensive range of apoptotic protein kinases belonging to the Src family, small G proteins, the Ras family, c-Jun, and the p38 mitogen-activated protein kinase (MAPK) pathways.[27] Furthermore, ROS are known to transmit cytoplasmic signals to the nucleus by influencing the activities of transcription factors that regulate gene expression. In counter-response to oxidative stress, cancer cells induce the transcription of antioxidant enzymes to regulate intracellular ROS levels.

Conversely, ROS have also been investigated for their therapeutic potential, especially in cancer management. High levels of ROS target cancer cells through the initiation of programmed cell death (PCD), facilitated by a group of proteases known as caspases, which are cysteine-dependent and aspartate-directed, culminating in the formation of apoptotic bodies. Monoclonal antibodies such as rituximab are used for the treatment of B cell lymphomas whose mechanism of action involves the suppression of BCL2 and p38MAPK signalling pathways, which in turn increases ROS levels and triggers apoptosis (Fig. 2).[28] The application of ROS as therapeutics is also extended to neurodegenerative diseases. The photodynamic therapy (PDT) is a strategy targeting diseases through controlled and localized ROS generation. In a report, photooxygenation of amyloid β (Aβ) was achieved using peptide-based porphyrin supramolecular self-assembly (PKNPs) for Alzheimer's disease (AD) treatment.[29] The Aβ-responsive structural transformation of PKNPs was designed for selective photooxygenation of Aβ enabling controlled ROS production. PKNPs as activatable photosensitizers offer targeted therapy with enhanced blood–brain barrier (BBB) permeability and Aβ-driven disassembly. Smart peptide-based metallo-nanodrugs were utilized for effective PDT with a high ROS generation capacity, making it a next-generation smart nanomedicine for cancer therapy.[30] Hypoxia

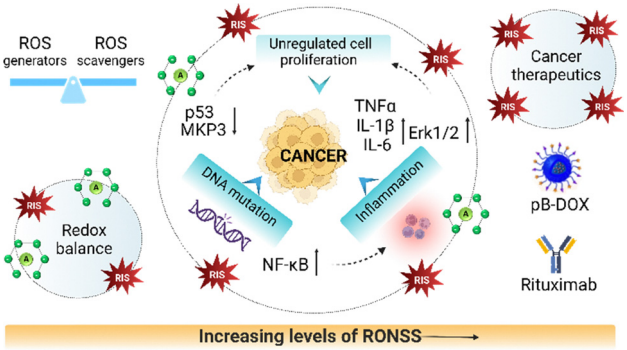

Fig. 2 Role of RONSS in the etiology of cancer. Upsurge in RONSS causes upregulation of cytokines and growth factors and downregulation of tumor suppressor genes, resulting in excessive cell proliferation while excessive RONSS can also be used therapeutically to annihilate cancer cells (created with https://www.biorender.com/).

has been observed in both cancer and neurodegeneration and thus development of probes for its detection is an emerging field.[31] Oxygen therapy has also been reported to act on many pathological aspects of AD such as Aβ metabolism, tau phosphorylation, neuroinflammation and neuronal apoptosis.[32] These advancements showcase the potential of controllable and localized ROS generation in various therapeutic applications.

RNS such as NO, nitrite (NO_2^-), nitrate (NO_3^-) and 3-nitrotyrosine and others are involved in cellular signalling, immune response, and vasodilation. Additionally, NO is instrumental in the immune system response mechanism to infections.[33] In the nervous system, NO functions as a neurotransmitter and is involved in the transmission of signals between neurons. Furthermore, $ONOO^-$ may exhibit antimicrobial properties and contribute to the immune response against pathogens.[34] A balanced synergy exists in the production of RNS, which is attributed to immune responses against the activation of macrophages in tumor cells, or to proinflammatory cytokines.

Unlike ROS and RNS which are often associated with oxidative stress and cellular damage, RSS have predominantly been recognized for their beneficial roles, particularly their antioxidant properties. Studies have shown a significant correlation between the expression of *trans*-sulfuration enzymes, namely cystathionine β-synthase (CBS) and cystathionine γ-lyase (CSE), which are integral to the endogenous production of H_2S, and lifespan.[35] Cysteine persulfidation serves as a protective mechanism against overoxidation induced by excessive ROS, and this process is conserved across various species, including mice and humans. H_2S is an essential signaling molecule in cellular processes and regulates numerous physiological functions such as blood vessel dilation, inflammation regulation, and neurotransmission.[36] H_2S influences protein function through a process known as sulfhydration, where it modifies cysteine residues in target proteins. While genetic studies suggest a potential relationship between RSS and senescence, the reason why reduced levels of RSS trigger cellular senescence remains unclear.[37] The chemistry and biological understanding of H_2S is still in its nascent stages, with several unresolved questions.

4. RONSS in diseases and their detection

RONSS, particularly ROS and RNS, play a crucial role in the pathogenesis of various diseases by inducing oxidative/nitrosative stress and causing subsequent biomolecular damage. The detection and therapeutic modulation of these species are crucial for devising advanced strategies to alleviate their deleterious effects.

4.1 Metals, RONSS and their implications in diseases

Metals play a pivotal role in numerous biological processes, nevertheless, an imbalance in metal homeostasis can instigate the production of ROS, leading to oxidative stress. Fe, while indispensable for physiological processes, can prove detrimental when present in excess as labile iron pool (LIP). Fe ions engage in the Fenton reaction with H_2O_2, culminating in the generation of highly reactive HO$^{\bullet}$.[38] Similarly, Cu^{2+} instigates oxidative stress by catalysing the Fenton-type reaction. In the presence of O_2^- or biological reductants such as ascorbic acid or GSH, Cu^{2+} is reduced to Cu^+ in a cyclic redox process. This results in the generation of HO$^{\bullet}$ through the decomposition of H_2O_2. Notably, both Cu and Fe have been shown to form inclusion complexes with Aβ peptides and proteins to accelerate their aggregation and produce excessive ROS, implicated in AD.[3,39] Ferroptosis/oxytosis, is an Fe-dependent form of cell death that involves lipid peroxidation by ROS produced by Fe^{3+}/Fe^{2+} redox cycle.[40,41] Transferrin receptor imports Fe as Fe^{2+}, reduced by Six Transmembrane Epithelial Antigen of Prostate 3 (STEAP3) to form lipid radicals (R$^{\bullet}$) and initiate lipid peroxidation. GSH, through the glutamate cysteine antiporter, plays a crucial role in regulating ferroptosis *via* GPX4 (Fig. 3).[11] Cuproptosis is a Cu-dependent cell death involves lipoylated enzymes accumulation and loss of Fe–S cluster proteins.[42] FDX1 converts Cu^{2+} to Cu^+, promoting cell death through dihydrolipoamide *S*-acetyltransferase (DLAT) lipoylation and Fe–S cluster inhibition. Cu^+ binds to lipoylated DLAT, triggering aggregation and cell death (Fig. 3). These metal ion-dependent forms of cell death underscore the intricate interplay between metal homeostasis, redox biology and cell fate highlighting their potential as therapeutic targets in various diseases.

4.2 RONSS in neurodegeneration

The brain is supplied with a substantial amount of oxygen (>20%, through blood supply) for its optimal function. It is susceptible to oxidative stress and subsequent damage due to relatively low levels of antioxidant enzymes and high levels of catalytic transition metals which trigger ROS and RNS. This vulnerability can lead to a variety of neurodegenerative disorders, including AD, PD, HD, and ALS.

4.2.1 AD. AD is a neurodegenerative disorder characterized by brain damage and is primarily attributed to the accumulation of senile plaques of Aβ and neurofibrillary tangles (NFT) of hyperphosphorylated tau.[43,44] Oxidative stress plays a crucial role in the progression of AD by causing neuronal damage and exacerbating amyloid aggregation and toxicity. It contributes to this pathology through the generation of ROS, promotion of neuroinflammation, disruption of mitochondrial function, calcium homeostasis imbalance, and the initiation of apoptotic cell death pathways (Fig. 4).[44–46] In addition to ROS, increase in the expression of neuronal (nNOS or NOS-1), cytokine-inducible (iNOS or NOS-2) microglial and endothelial (eNOS or NOS-3) NO isoenzymes have been observed. This can trigger inflammatory pathways and contribute to neuroinflammation, which is a characteristic feature of AD. Oxidative changes like protein nitration and nucleic acid modifications are observed in the AD brains.[47]

Elevated levels of oxidative stress in AD reduces antioxidants levels such as vitamins C and E, uric acid, SOD, CAT, GPX, which eventually affect neurons, contributing to cognitive impairment and memory deficits and as such many antioxidants are known to act as inhibitors of AD.

4.2.1.1 Probes targeting RONSS in AD. A multitude of probes have been deployed for the detection of diverse classes of RONSS abundant in the brain as biomarkers in AD. Concurrently, therapeutic interventions aimed at mitigating RONSS have become integral components of contemporary AD

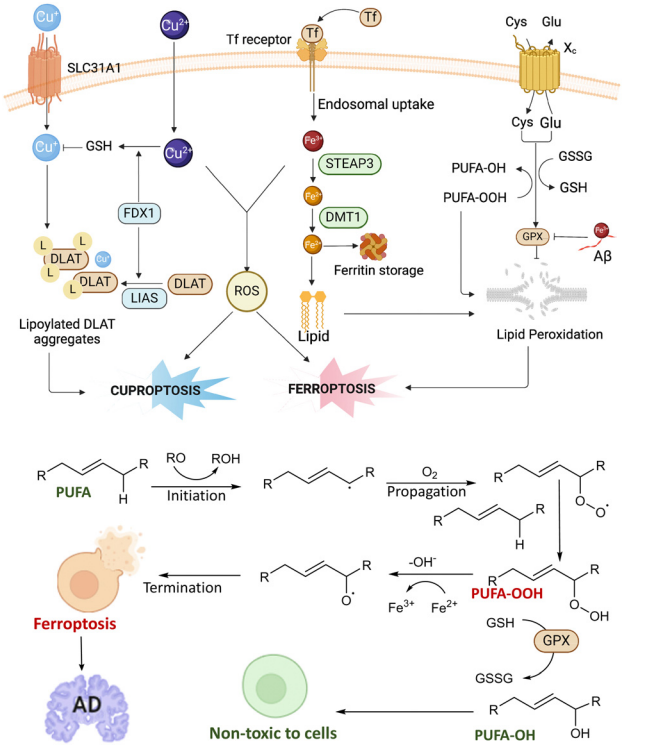

Fig. 3 Schematic shows the mechanism of ferroptosis, cuproptosis and their nexus with AD. Fe accumulation in cells aggravates the peroxidation of lipids which causes the Fe-dependent cell death, ferroptosis. The GSH/GPX4 axis regulates lipid peroxidation, preventing ferroptosis, while Aβ/Fe system reduces GPX4 levels. Cu mediates the lipoylation of DLAT protein whose aggregation leads to cell death in cuproptosis (created with **https://www.biorender.com/**). Lower panel shows the chain reaction involved in lipid peroxidation. Tf: transferrin, TNF α: tumor necrosis factor α, STEAP3: six-transmembrane epithelial antigen of the prostate 3, DMT1: divalent metal transporter 1, DLAT: dihydrolipoamide *S*-acetyltransferase, FDX1: ferredoxin 1, LIAS: lipoic acid synthase, SLC31A1: solute carrier family 31 member 1, PUFA: polyunsaturated fatty acid.

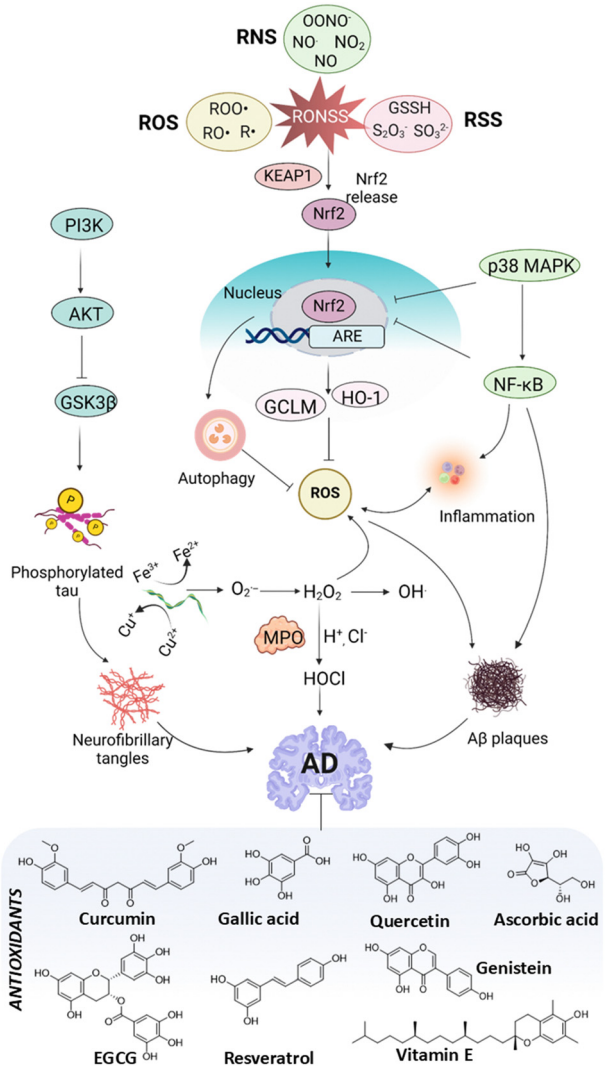

Fig. 4 Elevated levels of RONSS contribute to neurodegeneration. Activation of microglia and astrocytes releases enzymes such as inducible nitric oxide synthase (iNOS), NADPH oxidase (NOX) and inflammatory indicators such as tumor necrosis factor (TNFα), interleukins (IL-4, IL-5, IL-6, TGF-β), which result in neuronal death and neuroinflammation (created with **https://www.biorender.com**). Antioxidants act as potent AD inhibitors.

treatment paradigms. Probes often contain functional groups that react selectively with RONSS, leading to measurable changes in their fluorescence properties. For instance, some probes undergo oxidation, aggregation or cleavage in the presence of specific RONSS, resulting in a quantifiable fluorescent signal.[48] These chemical interactions allow for the accurate detection and quantification of RONSS levels within biological systems.[12] Fluorescent probes can identify target compounds through weak molecular interactions or chemical reactions. Typically, molecular fluorescent probes consist of a fluorophore, a linker, and a recognition group. Traditional design strategies offer optical recognition for detection by interacting with analytes, typically forming a lock-and-key type of interaction. However, activity-based fluorescent probes that function *via* chemical bonding are more ideal for real-time imaging of ROS and RNS. The main sensing mechanisms include photoinduced electron transfer (PeT), intramolecular charge transfer (ICT), fluorescence resonance energy transfer (FRET), excited-state intramolecular proton transfer (ESIPT), and aggregation-induced emission (AIE).[49]

In AD, different probes based on different mechanisms have been designed for detection of RONSS. HOCl produced in macrophages and phagocytes neutralize pathogens such as viruses and bacteria. The production of HOCl from H_2O_2 is catalysed by MPO enzyme. The overexpression of MPO, Aβ plaques and its inclusion complexes of Cu^{2+} and Fe^{3+} result in the production of excess HOCl in the brain, which aggravate oxidative stress and inflammation in AD, thus acting as a potential biomarker.[50] In this context, we have developed a molecular probe for the unambiguous detection of elevated HOCl levels in the brains of AD double transgenic mice (Fig. 5(a)).[8] The coumarin–morpholine conjugate (**CM2**) probe acts as a turn on fluorescent probe for the specific detection of HOCl produced and proximally localized with amyloid plaques. In the presence of HOCl, the non-fluorescent thioamide probe **CM2** undergoes regioselective transformation to fluorescent amide probe CM1 with remarkable selectivity and sensitivity (90-fold fluorescence enhancement, 0.32 quantum yield, and detection limit: 0.17 μM) (Fig. 5(b)). Confocal microscopy imaging validated the excellent detection capability of the probe in the cortex and hippocampus regions of the AD transgenic mice brain tissues (Fig. 5(c) and (d)). This study established and validated HOCl produced and proximally localized with amyloid plaques as a new combination biomarker with potential to be qualified for inclusion in the National Institute on Aging and Alzheimer's Association (NIA-AA) research framework 2024 designated list of biomarkers (ATN) for reliable AD diagnosis.

Aβ instigates the production of NOS in microglial cells, which in turn generates NO and $ONOO^-$. These RNS released from microglial cells damage biomolecules through nitrosylation causing neuronal dysfunction and cell death. In fact, an elevated levels of nitrosylated proteins were detected in the neurons located in the cortex and hippocampus regions of the AD patients' brains. This observation suggests the potential utility of $ONOO^-$ as a diagnostic marker for AD.[54] A dual-functional probe (**3-HF-Ome**) was developed for detecting $ONOO^-$ using the fluorescence property of 3-hydroxyflavone (3-HFs) that works *via* the excited state intramolecular proton transfer (ESIPT) mechanism (Fig. 5(e) and (f)).[51] ESIPT results in normal and phototautomeric species with distinct emissions upon excitation, which can be observed in the fluorescence emission spectra of 3-HF-OMe. The presence of $A\beta_{42}$ oligomers and aggregates with $ONOO^-$ results in distinct fluorescence emission by **3-HF-OMe**, demonstrating its robust sensing capabilities (Fig. 5(g)). Wang *et al.* developed BTNPO, an innovative two-photon fluorescent probe adept at tracking the distribution and alterations of Aβ aggregates and $ONOO^-$ *via* two distinct fluorescence channels.[55] BTNPO consists of a benzothiazole-naphthalene derivative, chosen for its structural similarity to thioflavin T, which serves as the recognition group for Aβ

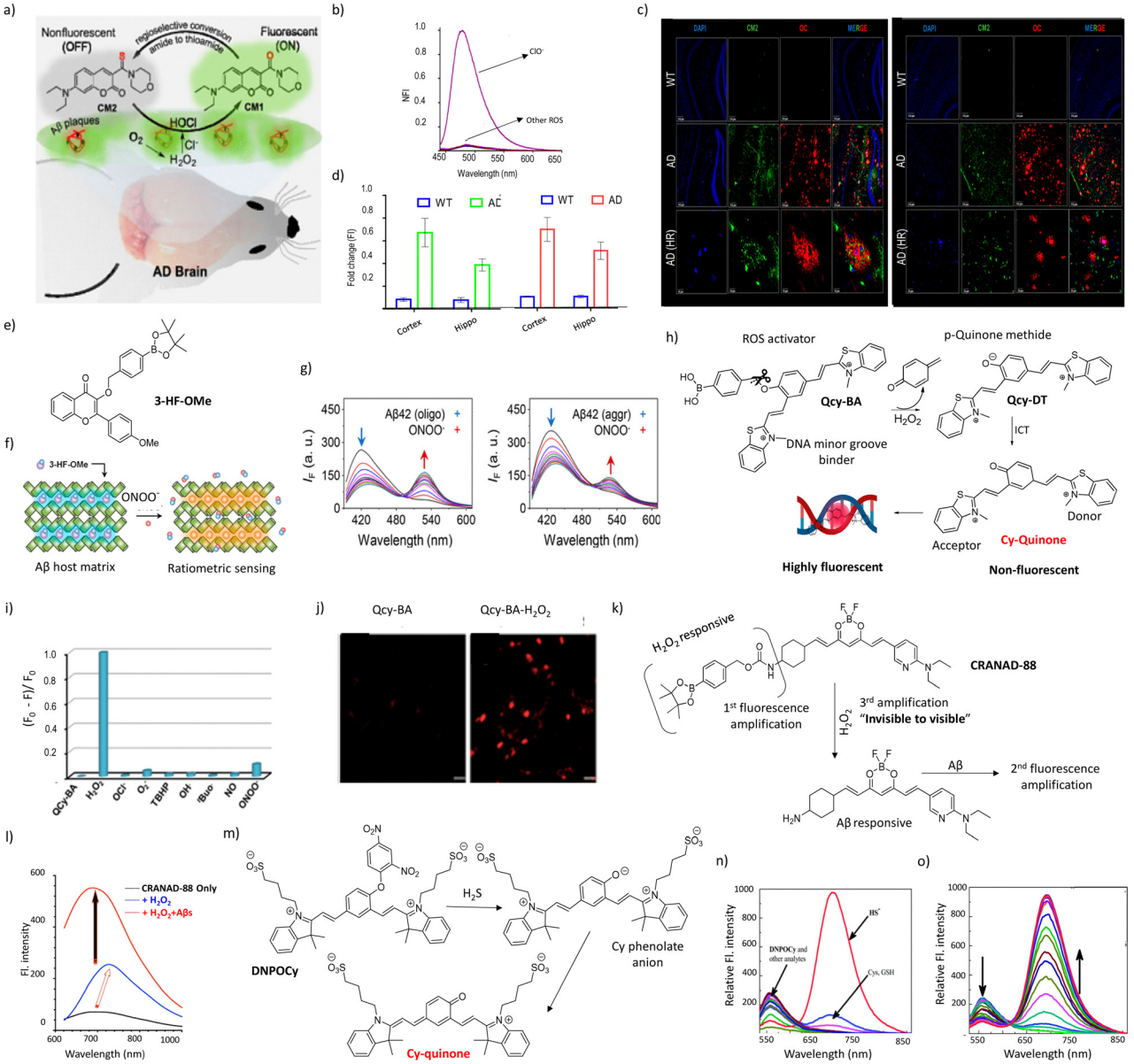

Fig. 5 Detection of RONSS and associated oxidative stress. (a) Structure of **CM2** and its HOCl detection mechanism. (b) Fluorescence response of **CM2** to various ROS. (c) Confocal microscopy images of hippocampus (left) and cortex (right) of the **CM2** administered WT and AD mouse brain and (d) corresponding quantification of HOCl (green) with Aβ plaques (red). Scale bar: 150 μm. Reproduced with permission from ref. 8. Copyright 2019 American Chemical Society. (e) Structure of **3-HF-OMe** and (f) its mechanism of sensing. (g) Fluorescence emission spectra of **3-HF-OMe** in presence of $A\beta_{42}$ oligomers and $A\beta_{42}$ aggregates in presence of $ONOO^-$. Reproduced with permission from ref. 51. Copyright 2018 American Chemical Society. (h) Schematic representation for the conversion of **QCy-BA** to QCy-DT in presence of H_2O_2. (i) Fluorescence response of **QCy-BA** to various ROS. (j) Fluorescence microscopy of MRC5 cells incubated with **QCy-BA** in absence and presence of H_2O_2. Scale bar: 20 μm. Reproduced with permission from ref. 9. Copyright 2016 Royal Society of Chemistry. (k) Schematic representation of the fluorescence amplification of **CRANAD 88** in response to H_2O_2 and Aβ. (l) Fluorescence response of **CRANAD-88** on addition of H_2O_2 and Aβ. Reproduced with permission from ref. 52. Copyright 2016 Springer Nature. (m) Conversion of **DNPOCy** to NIR emitting Cy dye in response to H_2S. Fluorescence response of **DNPOCy** on addition of different ROS (n) and H_2S (o). Reproduced with permission from ref. 53. Copyright 2014 Royal Society of Chemistry.

aggregates and oxindole which acts as the recognition group for $ONOO^-$. Through co-imaging the dynamics of Aβ aggregates and $ONOO^-$ levels in brain slices across various ages, it was revealed that elevated levels of $ONOO^-$ manifested earlier than Aβ aggregates in the brains of AD mice.

Stimuli-responsive fluorescent probes are widely utilized in detecting the physiological and pathological states of living systems. We have developed a boronic acid-functionalized quinone-cyanine probe (**QCy-BA**) in combination with AT-rich DNA (exogenous or endogenous cellular DNA), termed QCy-BA⊂DNA, acts as a stimuli-responsive Near-Infrared (NIR) fluorescence probe for measuring the cellular levels and homeostasis of H_2O_2.[4] The potential role of H_2O_2 in causing oxidative stress in AD is well established. Deposits of Aβ plaques, NFTs, and their metal-inclusions catalyse the production of $^{\bullet}OH$ from H_2O_2 through the Fenton reaction. Upon exposure to cellular

H_2O_2, **QCy-BA** transforms into QCy-DT, a one-donor, two-acceptor (D2A) system that binds to the cellular DNA and displays switch-on NIR fluorescence (Fig. 5(h)–(j)). **QCy-BA** can detect both normal and elevated levels of H_2O_2 produced by GOx-mediated oxidation of glucose, through EGF/Nox pathways, and post-genotoxic stress in primary and senescent cells. A curcumin analogue **CRANAD-88** was designed by coupling a CRANAD-58 as Aβ recognition moiety and borate as H_2O_2-selective chemical moieties for the detection of H_2O_2 in AD (Fig. 5(k)).[52] **CRANAD-88** detects H_2O_2 with NIR fluorescence (NIRF) in transgenic AD model APP/PS1 mice brain samples containing Aβ plagues (Fig. 5(l)).

In addition to ROS and RNS, emerging reports suggest a role for RSS, specifically H_2S, in neurological diseases. H_2S has been implicated in the regulation of memory in numerous studies, leading to a hypothesis that the characteristic memory decline in AD may be related to decreased levels of H_2S in the brain. There have been conflicting reports on reduced levels of free H_2S in AD patients as compared to healthy controls, however, alteration in the total sulfide concentrations (acid-labile and bound) was observed in AD patients.[56] We have developed a highly sensitive ratiometric NIR fluorescence and colorimetric probe, **DNPOCy** for H_2S detection, that reacts rapidly with H_2S in an aqueous medium to release the cyanine dye, Cy-quinone which displays NIR emission at λ_{em} = 555 nm (Fig. 5(m)–(o)).[53]

4.2.1.2 Therapeutic strategies targeting RONSS for mitigating AD. In the field of therapeutics, several molecules with RONSS scavenging properties have been developed as a therapeutic route towards AD. Aβ in the presence of redox-active metals such as Cu^{2+} and Fe^{3+} can produce ROS leading to oxidative stress. We have developed a peptidomimetic inhibitor **P6** combining a Cu-binding natural tripeptide of human origin, GHK, and hybrid peptoid with Aβ aggregation inhibition ability. (Fig. 6(a)).[57,58] **P6** complexes and maintain Cu^{2+} in a redox-dormant state preventing ROS production, exhibiting potent inhibition of Aβ and Cu^{2+} induced toxicity in cells. In a recent development, a series of short peptides (PNGln) conjugated with a dual-functional fluorophoric amino acid (NGln) was developed as anti-AD candidates, with the lead peptide, P2NGln, exhibiting strong Cu^{2+} affinity and stabilizing the ion in a redox-inactive state. P2NGln reduces ROS-mediated cytotoxicity induced by Cu^{2+}, and inhibits both Cu-dependent and independent $A\beta_{42}$ fibrillation and associated toxicity while suppressing liposaccharide-induced ROS and RNS production in microglial cells.[59] We have developed hybrid multifunctional modulators (HMMs) by combining the structural and functional elements of metal chelator clioquinol (Clq, one of the earliest drug candidates enter clinical trial for AD) and the natural antioxidant epigallocatechin gallate (EGCG) found in green tea.[47] We found that the lead HMM, TGR86 (Fig. 6(b)) complexes Cu^{2+} halting its redox cycle and averting the production of harmful ROS. TGR86 rescued PC12 cells from Aβ/Aβ-Cu^{2+}-induced neurotoxicity by preventing ROS generation. It protected biomolecules such as proteins, DNA, and lipids from damage inflicted by ROS. Furthermore, it disrupted the interaction of toxic Aβ species with mitochondria, thereby preventing mitochondrial damage. Inspired by GHK, We have designed small multifunctional modulators (MFMs) that modulate H_2O_2-induced ROS generation and quenches total nitrite concentration in LPS-treated cells (Fig. 6(c)–(e)).[60] While GHK and P6 modulate Cu^{2+}/Aβ-Cu^{2+}-associated toxicity, the lead analogue **MFM4** complexes both Cu^{2+} and Fe^{3+} in their free form or in their Aβ-bound states, disrupting their redox cycles and preventing excessive ROS production. This, in turn, ameliorates oxidative DNA damage and mitochondrial dysfunction and modulates Nrf2 protein signaling under oxidative stress conditions by eliminating toxic stress elements. In another natural product-inspired strategy, the berberine derivative, **Ber-D** (Fig. 6(f)) was developed, which has been shown to alleviate metal-dependent and independent Aβ toxicity.[10] Notably, **Ber-D** shows a remarkable ability to quench intracellular ROS, reduce protein oxidation, and inhibit DNA damage, lipid peroxidation, and mitochondrial damage, thereby protecting cells from apoptosis (Fig. 6(g)). Additionally, multi-targeted flavonoids with potent antioxidant properties have been shown to be effective against multiple pathways of AD.[61] We have designed synthesized small molecules with the capability to modulate the neuroinflammatory pathway. A small molecule, **M3**, (Fig. 6(h)) rationally designed by integrating pharmacophores for metal chelation, antioxidant onto $A\beta_{42}$ aggregation modulating naphthalene monoimide (NMI) scaffold was found to modulate metal dependent Aβ toxicity and reduce oxidative stress, as monitored by the Nrf2 signalling pathway.[62] **M3** effectively reduces microglial hyperactivation and neuroinflammation as monitored by bio-AFM analysis (Fig. 6(i)).

We designed and synthesized bipyridyl-based multifunctional modulators showing ROS and RNS scavenging properties, as examined from *in vitro* and in cellulo studies.[63] In SH-SY5Y cells, ROS was generated using H_2O_2, wherein the lead dopamine functionalized bipyridyl **compound 5** (Fig. 6(j)) effectively scavenged ROS, and rescued cells from oxidative stress and nitrosative stress (Fig. 6(k)). Neuroinflammation becomes a significant factor under oxidative stress conditions and its modulation is a major therapeutic approach in AD.[69] Ferroptosis and AD exhibit common pathological characteristics, which include an abnormal accumulation of Fe, elevated levels of ROS, increased lipid peroxidation, and diminished levels of antioxidant enzyme GPX4. The natural polyphenol, tannic acid (**TA**), a known antioxidant offers a comprehensive approach to simultaneous mitigation of ferroptosis and AD.[11] **TA** was identified as a Fe-chelator, ROS scavenger, and a potent inhibitor of $A\beta_{42}$ and tau aggregation. TA effectively modulates Fe-dyshomeostasis, harmful ROS, highly toxic Fe-induced $A\beta_{42}$ aggregates, inhibits mitochondrial damage, and activates Nrf2 (Fig. 6(l)) and thereby combating AD. In addition to inhibiting ferroptosis through conventional Fe-chelation and preventing ROS production and lipid peroxidation, **TA** binds to the activator site of GPX4 (Fig. 6(m)), enhancing the activity and cellular levels of the enzyme (Fig. 6(n)), thereby strengthening the inherent antioxidant mechanism. The combined approach of Nrf2-GPX4 activation and ferroptosis inhibition introduces a conceptually novel and integrated strategy for effectively targeting the GPX4-ferroptosis-AD axis to tackle AD pathology. The dual therapeutic nature of polyphenols inspired the design and synthesis of gallic acid-CDP hybrids where the lead molecule, **GCTR** synergistically combats both ferroptosis and

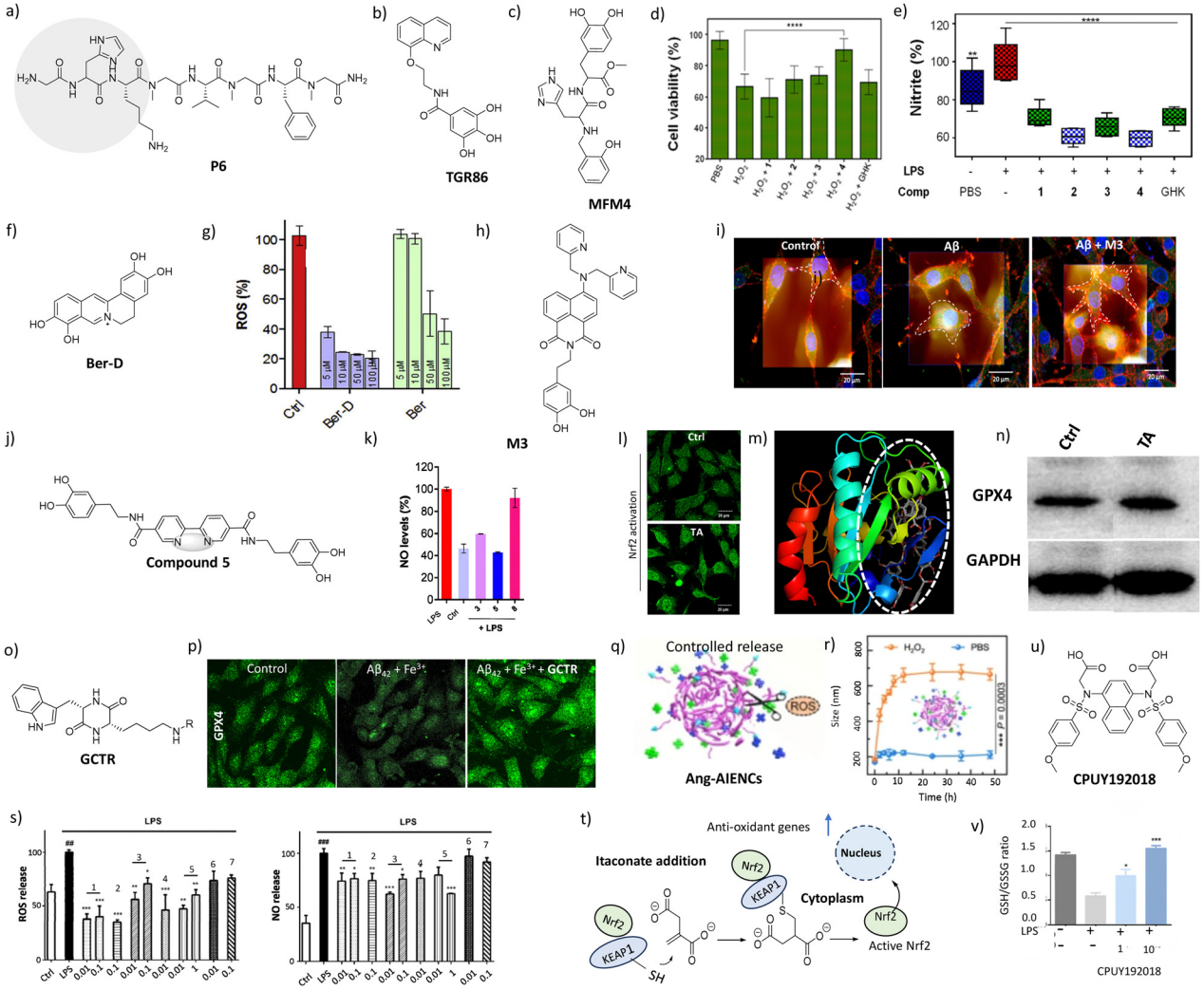

Fig. 6 Therapeutic strategies to modulate oxidative and metal dyshomeostasis in AD. Structure of (a) **P6**, (b) **TGR 86** (c) **MFM-4**. (d) In cellulo ROS quenching assay of MFM 1-4 and GHK. (e) % Nitrite concentration measured in cell media upon treatment with MFM 1–4 or GHK. Reproduced with permission from ref. 60. Copyright 2019 American Chemical Society. (f) Structure of **Ber-D**. (g) Quantification of ROS generation by DCFDA assay in PC12 cells incubated with $A\beta_{42}$, Cu^{2+} and **Ber-D**. Reproduced with permission from ref. 10. Copyright 2020 Cell Press. (h) Structure of **M3**, (i) Microglial activation monitored by both Bio-AFM and confocal microscope reproduced with permission from ref. 62. Copyright 2022 American Chemical Society. (j) Structure of lead bipyridyl multifunctional modulator, **compound 5**, (k) NO levels (RNS) by Griess assay reproduced with permission from ref. 63. Copyright 2022 Royal Society of Chemistry. (l) Nrf2 activation by **TA**. Scale bar: 30 μm (m) **TA** binds to activator site of GPX4. (n) Western blot to monitor enhancement in GPX4 levels in presence of **TA**. Reproduced with permission from ref. 11. Copyright 2023 Royal Society of Chemistry. (o) Structure of **GCTR**. (p) IF imaging to monitor decline in GPX4 levels in presence of Aβ + Fe^{3+} and its enhancement on co-treatment with **GCTR**. Scale bar: 25 μm. Reproduced with permission from ref. 64. Copyright 2024 Elsevier. (q) The co-assembly of nanodrug Ang-AIE NCs, (r) Size change of NCs treated with PBS and H_2O_2 for various times. Reproduced with permission from ref. 65 Copyright Nature (s) Gracilin A derivatives decreased ROS and NO produced by microglia. Reproduced with permisiion from ref. 66. Copyright American chemical society. (t) **Itaconate** acts as a crucial anti-inflammatory metabolite, which engages Nrf2 to modulate type I interferons and limit inflammation. Adapted from ref. 67. Copyright 2018 Springer Nature (u) Structure of **CPUY192018**. (v) Ratio of GSH/GSSG were measured in HK-2 cells. Reproduced with permission from ref. 68. Copyright 2019 Elsevier.

amyloid toxicity (Fig. 6(o)).[64] **GCTR** enhances the expression of GPX4 (Fig. 6(p)) and modulates Fe^{3+}-induced liquid–liquid phase separation of tau, thereby fostering the development of small molecule-based novel therapeutics for AD. Furthermore, a polycatechol **PLDP**, comprising L-DOPA, was designed to possess antioxidant, anti-amyloid aggregation, and ferroptosis inhibition properties. Interestingly, while L-DOPA itself acts as a pro-oxidant in the presence of Fe, **PLDP** functioned as an antioxidant.[70]

A near-infrared-II aggregation-induced emission (AIE) nanotheranostic was engineered for targeted AD therapy. Upon activation by ROS, the release of two therapeutic AIE molecules was precisely controlled (Fig. 6(q)).[65] One molecule disrupted Aβ fibril formation, degraded existing fibrils and prevented reaggregation while the other scavenged ROS (Fig. 6(r)), restored redox balance thereby reversing neurotoxicity and enhancing cognitive function in a female AD mouse model. We present a polydopamine–ruthenium (PDA–Ru) nanosystem, which functions concurrently as a near-infrared photothermal therapy (PTT) agent, ROS scavenger, and H_2O_2 catalyst. This multi-functional approach holds promise as a therapeutic strategy for AD

and other neurodegenerative disorders.[71] Gracilin A derivatives, synthesized *via* pharmacophore-directed retrosynthesis, have demonstrated significant neuroprotective properties (Fig. 6(s)) They were particularly effective in modulating the expression of antioxidant genes (CAT, GPx, SODs, and Nrf2), reducing cytokine release (IL-1β, IL-6, GM-CSF, TNF-α) and other ROS/RNS, highlighting their potential as promising candidates for AD therapy.[66] The critical role of oxidative stress in AD has been recognized by researchers recently, and natural antioxidants have been demonstrated to have anti-AD activity in animal models, such as Ginkgo biloba extract, soy isoflavones, lycopene, and so on.[72] In the field of cancer therapeutics too, the development of novel tools has led to the utilization of nonenzymatic antioxidants, activators of Nrf2, inhibitors of NOX, and vitamins, as oxidative stress plays a role in the progression of cancer. For example, fumaric acid esters serve as Nrf2 activators that operate by modifying sensor cysteines of KEAP1, such as dimethyl fumarate (DMF). DMF operates by alkylating Cys151 of KEAP1, thereby disrupting the association between KEAP1 and Nrf2. The endogenous metabolite itaconate is often necessary for the activation of Nrf2, which operates *via* the alkylation of KEAP1. Itaconate acts as a critical anti-inflammatory metabolite, which engages Nrf2 to modulate type I interferons and limit inflammation (Fig. 6(t)).[67] The therapeutic efficacy of CPUY192018, a small-molecule inhibitor of the KEAP1-Nrf2 pathway in renal inflammation was evaluated. CPUY192018 significantly activates the Nrf2-based cytoprotective system and thus, protects the kidney from inflammatory injury (Fig. 6(u) and (v)).[68] Expanding the use of the dicyanomethylene-4*H*-chromone (DCM) chromophore, a novel NIR theranostic prodrug, DCM-S-CPT, for cancer chemotherapy in mice was explored making use of the abundance of the antioxidant GSH in cancer cells.[73] DCM-S-CPT links the DCM fragment to the camptothecin (CPT) drug through a disulfide linker, suppressing both fluorescence and cytotoxicity. However, cancer cells with excess GSH selectively cleave the disulfide bond, releasing the cytotoxic drug and the fluorophore from PEG-PLA-loaded nanoparticles. The production of ROS by NOX is accompanied by the formation of SO_2^-. Inflammation-triggered macrophages generate NO, which combines with SO_2^- to form $ONOO^-$, aiding in tumor cell death. Tumor cells express NOS isoforms, affecting progression based on type and stage. Human colorectal cancer and inflammatory diseases link inducible iNOS activity with p53 alterations, suggesting RNS trigger cancer-related gene mutations. Research using iNOS knockout mice implies NO from iNOS plays a role in melanoma carcinogenesis initiation and promotion.[74] Besides ROS and RNS, the association of RSS with oxidative stress arises from their consumption of thiols, raising ROS levels directly or indirectly. The selective oxidation holds promise for antimicrobial and cancer therapies.[75]

4.2.2 Other neurodegenerative disorders. Parkinson's disease (PD) is characterized by the degeneration of dopaminergic neurons in the substantia nigra and the accumulation of α-synuclein inclusion bodies known as Lewy bodies. The substantia nigra in PD patients exhibits elevated levels of oxidized lipids, proteins, and DNA, as well as reduced levels of GSH. Post-mortem analysis of brain tissue from PD patients revealed oxidative stress which results in increased levels of 4-hydroxyl-2-nonenal (HNE), a product of lipid peroxidation, carbonyl modifications of soluble proteins, and oxidation products of DNA and RNA (8-hydroxy-deoxyguanosine and 8-hydroxy-guanosine).[76] Amyloid Lateral sclerosis (ALS) involves oxidative stress-induced damage to proteins, lipid peroxidation, and DNA/RNA oxidation. Oxidative stress biomarkers like malondialdehyde (MDA)-modified protein, 8-hydroxy-2′-deoxyguanosine (8-OHdG) in DNA, and lipid peroxidation products are found elevated in ALS patients' urine, cerebrospinal fluid, and blood.[77] The mitochondrial dysfunction and elevated levels of ROS and RNS are evident in ALS. In patients with ALS, the H_2S levels in the spinal fluid is elevated (7.53 mg L^{-1}), in comparison to the control group (3.64 mg L^{-1}).[78] An increase in the brain H_2S has also been observed in ALS mouse models. Various reports document oxidative stress to be a significant contributor to Hungtington's disease (HD), an autosomal dominant, fully penetrant neurodegenerative disorder caused by a mutant huntingtin (mHTT) protein. Markers of oxidative stress like 8-OHdG, products of protein carbonylation, 3-nitrotyrosine, 4-hydroxynonenal and isoprostanes have been shown to be elevated in HD.[79]

4.2.2.1 Probes targeting RONSS in other neurodegenerative disorders. A dual-responsive fluorescent probe **Mito-VS** possesses high mitochondrion-targeting capabilities and can simultaneously measure mitochondrial viscosity and H_2S (Fig. 7(a)).[80] Mito-VS is initially nonfluorescent due to free intramolecular rotation between dimethylaniline and pyridine, but an increase in viscosity restricts this rotation, resulting in the release of intense red fluorescence. Liu *et al.* engineered **Mito NIRHV**, a near-infrared (NIR) fluorescent probe, to discern mitochondrial viscosity and H_2O_2 levels in the brains of PD mice (Fig. 7(b)).[81] The probe consisted of a *p*-pinacolborylbenzyl moiety which has high selectivity toward H_2O_2, a quaternarized quinoline unit for targeting mitochondria and a lipophilic π-conjugated thiophene-bridge extending NIR emission and a twistable ethylene responding to environmental viscosity. Huang *et al.* devised **BT-NH**, a fluorescent probe meticulously crafted for the specific and remarkably sensitive detection of NO within the brains of PD animal models (Fig. 7(c)). Its structure was inspired from diaminofluorescein and benzobis(1,2,5-thiadiazole) structures which harbour precision and sensitivity for NO.[82] Liu *et al.* pioneered **NIR-PNs**, a class of near-infrared probes capable of ultra-fast (within seconds) and highly selective detection of $ONOO^-$ across various PD animal models, underscoring their utility in rapid and specific detection assays (Fig. 7(d)).[83] For synthesizing **NIR-PNs**, dicyanoisophorone-based NIR fluorophore with a donor–π–acceptor structure was chosen for its biocompatibility, NIR emission, and photostability whereas *p*-aminophenol receptors were integrated as $ONOO^-$ reactive sites. Upon reacting with $ONOO^-$, *p*-aminophenol groups cleave to release *p*-benzoquinone, restoring the fluorescence of the probe. **Cu_xO nanoparticle** clusters (NCs) were developed to functionally mimic the activities of SOD, CAT and GPX4, which inhibited neurotoxicity in a cellular model of PD (Fig. 7(e)).[76] RNS contribute to lipid peroxidation and protein dysfunction through the formation of *S*-nitrosothiols, impairing the brain function in PD patients.[84] A decrease in the levels of H_2S is observed in the striatum and plasma of PD animal models.[85]

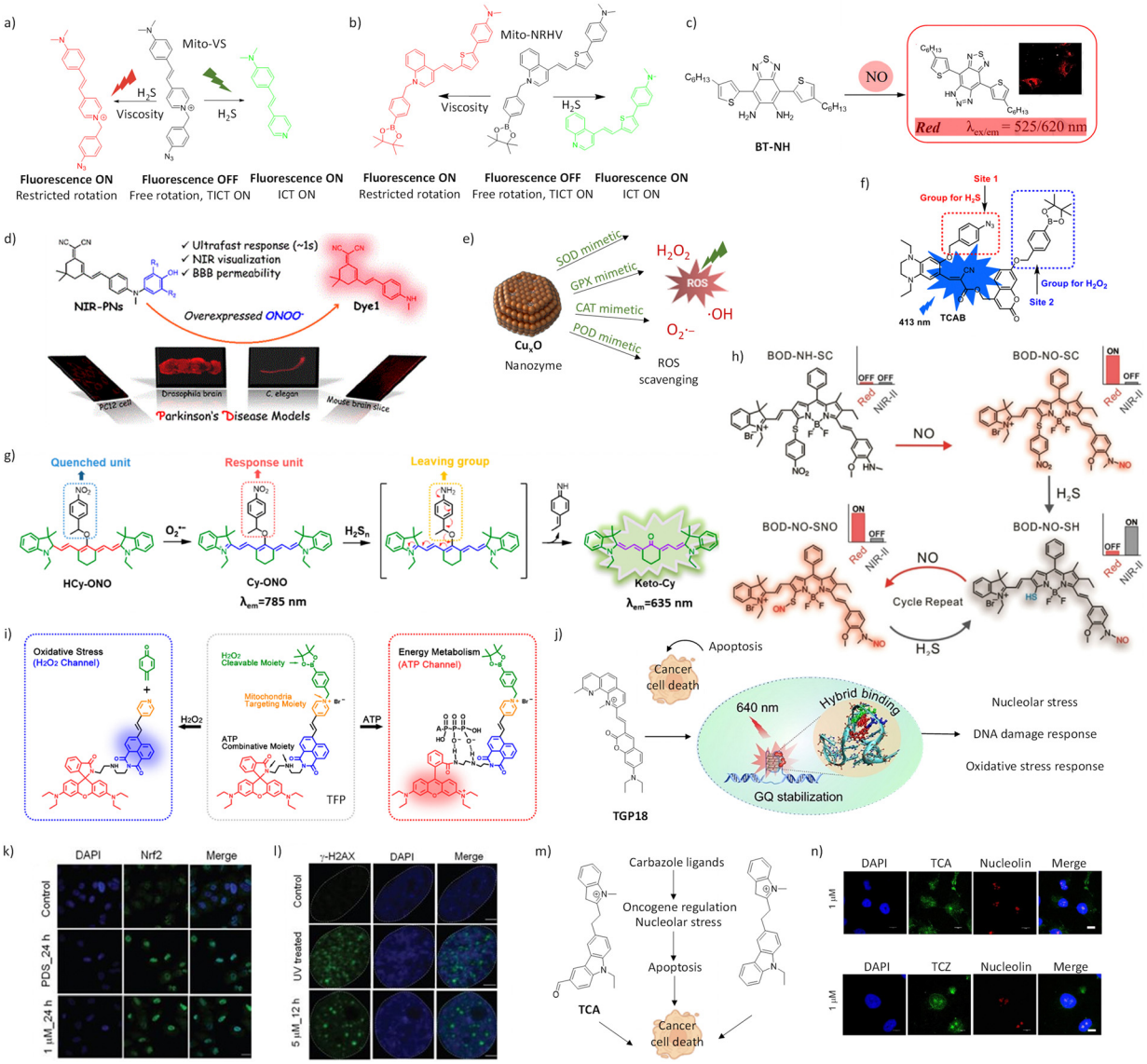

Fig. 7 (a) Design of dual-responsive fluorescent probe **Mito-VS** for detection of viscosity and H_2S. Reproduced with permission from ref. 80. Copyright 2018 American Chemical Society. (b) Design of dual-responsive fluorescent probe **Mito-NRHV** for detection of viscosity and H_2S. Reproduced with permission from ref. 81. Copyright 2020 Royal Society of Chemistry. (c) Design of **BT-NH** for the specific detection of NO within the brains of PD animal models. Reproduced with permission from ref. 82. Copyright 2019 Elsevier. (d) Design of **NIR-PNs**, a class of near-infrared probes for ultra-fast and highly selective detection of $ONOO^-$ across various PD animal models. Reproduced with permission from ref. 83. Copyright 2020 American Chemical Society. (e) Design of **Cu_xO nanoclusters**. Reproduced with permission from ref. 76. Copyright 2019 American Chemical Society. (f) Design strategy of **TCAB** for the precise detection of H_2S and H_2O_2 simultaneously. Reproduced with permission from ref. 86. Copyright 2020 American Chemical Society. (g) Design strategy for **HCy-ONO** that offers dual turn-on fluorescence responses for H_2Sn and $O_2^{\bullet -}$ in separate windows. Reproduced with permission from ref. 87. Copyright 2019 American Chemical Society. (h) Design strategy for **BOD-NH-SC**, an (ESIPT)-based 'AND' logic system probe, tailored for imaging thiols and $ONOO^-$ in cellular environments. Reproduced with permission from ref. 88. Copyright 2021 Wiley. (i) Design strategy for **TFP** for simultaneous determination of mitochondrial H_2O_2 and ATP changes in two well-separated fluorescence channels. Reproduced with permission from ref. 89. Copyright 2020 American Chemical Society. (j) Structure of **TGP18** and schematic showing its binding to GQ and subsequent cancer cell death. (k) Immunofluorescence images of A549 cells showing nuclear translocation of Nrf2 (green) upon treatment with TGP18. Scale bar: 10 μm. (l) Immunofluorescence images to assess DNA damage response (DDR) as a result of treatment with **TGP18** or UV exposure. Reproduced with permission from ref. 75. Copyright 2020 Ivyspring International Publisher. Reproduced with permission from ref. 77. Copyright 2020 Ivy spring International Publisher. (m) Structure of **TCA** and **TCZ** and their dual targeting nature causing cancer cell death. (n) Localization of **TCA** and **TCZ** (green) in MDAMB-231 cells by colocalizing with the Alexa 647-conjugated Nucleolin (red) antibody at 1 h. Reproduced with permission from ref. 86. Copyright 2022 American Chemistry Society.

The implication of RONSS with diverse pathological role is also evident in HD, Wilson's disease, psychiatric ailments, and schizophrenia, showcasing diverse roles.

4.2.2.2 Therapeutic strategies for mitigating RONSS in other neurodegenerative disorders. A study on high-dose antioxidant therapy combining vitamin C (3000 mg per day) and vitamin E

(3200 IU per day) suggests this approach may slow the progression of PD.[90] A multicenter, randomized, placebo-controlled, double-blind trial with parallel-group and dosage-ranging design further investigated the impact of Coenzyme Q10, an endogenous antioxidant at 300, 600, and 1200 mg daily compared to placebo wherein a dose-dependent improvement of physiological symptions was observed.[91] Intraventricular injections of iron chelators desferrioxamine and deferasirox were shown to prevent dopamine depletion in the striatum in a 6-OHDA rat model of PD.[92] In MPTP-induced mouse models, melatonin administration helped protect the nigrostriatal pathway from oxidative stress, neurotoxicity, and degeneration caused by the toxin, with similar findings in 6-OHDA models.[93] BN82451, a brain-penetrable compound for Huntington's disease, exhibits neuroprotective effects by safeguarding mitochondria against oxidative damage.[94] Another innovative antioxidant, XJB-5-131, which targets mitochondria, was found to substantially reduce mitochondrial DNA oxidative damage and slow disease progression in Huntington's disease animal models.[95] Dietary flavonoids like rutin, myricetin, and hesperidin also show benefits in Huntington's disease by activating the neuroprotective and cytoprotective Nrf2 pathways.[79]

In ALS mouse models, resveratrol, a SIRT1 activator, provided mitochondrial protection and symptomatic improvement.[96] Furthermore, a novel acylaminoimidazole derivative, WN1316, which selectively reduces oxidative stress-induced cell death and inflammation by upregulating Nrf2 and boosting GSH, showed efficacy in enhancing motor function and extending survival in SOD1H46R- and SOD1G93A-transgenic mice.[97] Edavarone (MCI-186) acts a free radical scavenger of both oxidative and nitrosative stress and exhibits therapeutic potency against ALS.[98]

4.3 RONSS in cancer

The high mitochondrial metabolism observed in cancer cells leads to an increase in RONSS levels, which in turn promotes tumorigenesis and the accumulation of mutations, thereby facilitating faster growth and spread. The role of ROS in tumorigenesis was first proposed in the 1990s.[99] In p53-heterozygous mice, the deletion of Brca1 results in increased ROS and the formation of mammary tumors.[100] The control of oxidative stress by Brca1 involves Nrf2. Growth factors and cytokines such as Interferon (IFN), Tumor Necrosis Factor (TNF), and macrophages stimulate the production of H_2O_2 and NO in tumor cells. The activation of Erk1/2 by ROS enhances survival, growth, and motility in various cancers including ovarian, breast, melanoma, and leukemia. The Kirsten rat sarcoma viral oncogene homolog (K-Ras) triggers the activation of the MAPK/Erk1/2 pathway, which is linked to cell proliferation. Ovarian cancer cells with high levels of ROS exhibit elevated Erk1/2 due to persistent ubiquitination and loss of MKP3, thereby enhancing Erk1/2 activity.[101]

4.3.1 Probes targeting RONSS in cancer. Given the high oxidative stress in cancer cells, several probes have been developed to detect specific ROS overexpressed in cancerous cell lines. Wang *et al.* devised a fluorescent probe **TCAB**, tailored for the precise detection of H_2S and H_2O_2 simultaneously in HeLa cells and zebrafish (Fig. 7(f)).[86] Comprising a synergistic duo of short-wavelength emitting coumarin HCB and long-wavelength emitting fluorophore TQC, **TCAB**'s design integrated benzyl boronic ester and azide functional groups, strategically positioned as sensing units for H_2O_2 and H_2S, respectively. To elucidate the roles of H_2O_2/SO_2 in oxidative stress, Wang *et al.* developed a spectral-response-separated fluorescent probe, **HCy-ONO**, to study the interaction of H_2S and $O_2^{\bullet-}$ in living cells and *in vivo* (Fig. 7(g)). **HCy-ONO** offers dual turn-on fluorescence responses for H_2S_n and $O_2^{\bullet-}$ in separate windows, minimizing spectral overlap interference. Using this probe, we monitored H_2S_n and $O_2^{\bullet-}$ levels in living cells under continuous and intermittent hypoxic conditions.[87] **BOD-NH-SC**, an (ESIPT)-based 'AND' logic system probe was developed, tailored for imaging thiols and $ONOO^-$ in cellular environments (Fig. 7(h)).[88] In macrophages, the presence of endogenous NO triggered **BOD-NH-SC** to emit intense red fluorescence, with comparatively weak NIR fluorescence. However, upon incubation with fluvastatin-stimulated macrophages which is known to induce endogenous H_2S production, the fluorescence signal in the NIR-II channel surged by 16.2-fold compared to untreated cells. Tian *et al.* introduced a two-photon fluorescence-lifetime-based probe (**TFP**), capable of concomitantly assessing H_2O_2 and ATP levels within mitochondria (Fig. 7(i)).[89] **TFP** offered real-time imaging and the simultaneous determination of mitochondrial H_2O_2 and ATP changes in two well-separated fluorescence channels without spectral crosstalk. Additionally, You *et al.* designed **MPIBA**, a dual-response probe for SO_2/ClO^-.[102] The ability of SO_2 to act as both oxidizing and reducing agent reveals its dual effects during oxidative stress *via* its ability to exhibit both oxidative and antioxidative property in cells.

4.3.2 Therapeutics utilizing RONSS in cancer. The strategic use of ROS as a therapeutic modality for targeting and eradicating cancer cells has been a focus of scientific investigation. A responsive nanosystem, UCNPs@Cu–Cys–GOx (UCCG) was designed that react with glucose to switch off the nutrient source for achieving starvation treatment and supplying H_2O_2 to boost cancer therapy.[103] A ROS-responsive doxorubicin prodrug (pB-DOX) was developed for tumor targeting using boronate moieties, loaded with indocyanine green (ICG) and modified with liposomes, offering precise drug release at tumor sites for effective cancer PDT (Fig. 2).[104] As a novel anticancer drug, b-Lap can rapidly produce a large amount of ROS by catalysing NQO1 to induce cancer cell apoptosis. Lysozyme-gold nanoclusters/rose bengal conjugate (Lys-Au NCs/RB) was introduced as a photosensitizer for antibacterial and antibiofilm treatment, impeding bacterial growth upon white LED irradiation.[105] Recently, we discovered a theranostic probe for topology-selective recognition of oncogene-specific G-quadruplex (GQ) structures. **TGP18** binds to BCL2 GQ through a unique hybrid loop stacking and groove binding mode (Fig. 7(j)).[75] The selective binding of TGP18 to BCL2 GQ resulted in a turn-on far-red fluorescence response and anticancer activity, demonstrating its potential for GQ-targeted cancer theranostics. Targeting BCL2 GQ caused genome instability through the induction of oxidative stress and DNA damage, rendering lung cancer cells sensitive to **TGP18**. Nrf2 translocation as an

oxidative stress response (OSR), nucleolar stress, oxidative DNA damage (8-oxo-7,8-dihydroguanine) in the GQ forming promoter sequence, and other associated mechanisms recapitulated the features of oxidative stress as a possible mutual pathway for DNA damage response (DDR), cell cycle arrest, and apoptosis induced by **TGP18** (Fig. 7(k) and (l)).[106–108] Overall, the intervention through GQ-mediated lethality by TGP18 has translated into excellent lung cancer activity in both *in vitro* 3D spheroid culture and *in vivo* xenograft model of lung cancer. We reported carbazole-based monocyanine ligands **TCA** and **TCZ** (Fig. 7(m)) to enhance GQ selectivity at oncogene promoter levels (BCL2 and C-MYC, respectively), visualize GQ structures in live cells with demonstrated therapeutic potential.[108] **TCA**/**TCZ**-induced nucleolar stress (Fig. 7(n)) and also impaired the synthesis of rRNA genes involved in ribosome biogenesis. This study revealed dual-targeting GQ binding ligands with synergistic arrest of oncogene overexpression and rRNA biogenesis which resulted in inhibition of cell proliferation and induction of apoptosis.

4.4 RONSS in inflammation

The immune system initiates a defense mechanism in response to any pathological assault, including inflammation. ROS is involved in regulating the inflammatory response through key regulators such as Nrf2, NF-κB, and TNFR1 pathways. In disease conditions, mitochondrial ROS triggers the activation of tissue macrophage inflammasomes, which mediate inflammation. It has been reported that NALP and NLRP inflammasomes are regulated by mitochondrial ROS through MAPK/Erk1/2 pathways.[109] ROS also regulates the infiltration of cells to the site of inflammation by facilitating the extravasation of inflammatory macrophages. A gradient of H_2O_2 created around the wound signals the infiltration of macrophages to the injury site. Endothelial junctions serve as barriers to the extravascular infiltration of inflammatory cells. ROS regulates occludin interactions through GSH. The recruitment of neutrophils is regulated by ROS through the regulated expression of IL1β. Microbes increase extracellular ROS, triggering IL1β expression to infiltrate neutrophils and clear the microbial load. There are a few reports suggesting that mitochondrial ROS regulates endothelial cell migration and angiogenesis, which are essential for the inflammatory response. The regulation of inflammation by ROS and oxidative stress is mediated by various redox-sensitive transcription factors and inflammatory cytokines. NF-κB, a redox-sensitive transcription factor, is involved in regulating inflammatory processes in response to ROS. Mitochondrial ROS is known to promote TNFα-mediated NF-κB activation and inflammatory response.[110] NOX-dependent ROS regulates the differentiation of macrophages to M2 phenotypes and continues the production of NO, which is required for the bactericidal activity of M2 macrophages. Tang *et al.* designed an activatable fluorescent nanoprobe (**TPE–IPB–PEG**) with AIE emission characteristics that were used to accurately image $ONOO^-$ at the site of inflammation in bacterially infected mice (Fig. 8(a) and (b)).[111] **TPE-IPB** consists of a tetraphenylethene (TPE) moiety as an AIEgen, an imine group as an emission mediator, and a phenylboronate as a recognition site for $ONOO^-$. Formulated with a lipid–PEG matrix, TPE-IPB nanoprobes (**TPE-IPB-PEG**) are non-fluorescent in aqueous solution but emit intense yellow fluorescence upon reaction with $ONOO^-$ at pH 7.4. Subsequently, Wang and coworkers introduced a fluorescent probe, **PAM–BN–PB** for the rapid imaging of H_2O_2 in mice afflicted with peritonitis, utilizing phenanthroimidazole, benzonitrile, and benzyl boronic ester components (Fig. 8(c)).[112] Additionally, they developed **HOTN**, a tetrastyrene-based AIE fluorescent probe capable of visualizing signals of HOCl in mouse models of peritonitis, arthritis, and liver cancer.[113] In another study, **Pinkment**, a functionalized synthetic derivative of peroxyresorufin-1, was developed aimed at visualizing $ONOO^-$ in LPS-induced peritonitis mouse models, enabling assessment of the therapeutic efficacy of indomethacin using resorufin as the fluorophore and a boronic ester as the $ONOO^-$ recognition moiety (Fig. 8(d)–(f)).[114] Furthermore, Chang *et al.* presented **MITO-CC**, a two-photon ratiometric fluorescence probe for the detection of $ONOO^-$ in cells and inflammation mouse models (Fig. 8(g)).[115] **MITO-CC** featured a rhodamine derivative for $ONOO^-$ recognition and coumarin for energy donation, enabling ratiometric detection of $ONOO^-$.

4.5 RONSS in cardiovascular, liver and kidney disease

Physiologically, the RONSS regulates the activities of vascular smooth muscle cells, influencing their contraction, relaxation, and development. Recent studies suggest that ROS may directly affect cardiac contractility, in addition to its indirect effects. There are reports indicating that ROS could enhance the inotropic effect of substances such as ET-1 by activating redox signalling pathways like Erk1/2. The activation of MAPK, particularly p38 MAP kinase, may precede the overproduction of ROS, which is associated with heart failure.[119] ROS plays a significant role in coronary artery disease by mediating the creation of oxidized LDL and activating matrix metalloproteinases (MMP), leading to plaque rupture. An increase in ROS levels due to D-amino acid oxidase may result in systolic heart failure without ventricular hypertrophy in rat hearts. Furthermore, ROS contributes to the formation of thrombus and other cardiovascular diseases. Patients with heart failure have been found to exhibit reduced NO production, increased nitrotyrosine formation, and increased iNOS expression.[120] The role of RSS in cardiovascular disease remains unclear. However, down-regulated H_2S pathways have been implicated in vascular disorders.

The kidney and liver are organs that are highly susceptible to oxidative damage. During damage, there is a surge in ischemia-related RONSS components such as $ONOO^-$ and HOCl, while antioxidant enzymes decline. This phenomenon is observed in renal tissue following ischemia and nephrotoxicity, as well as in sepsis-induced kidney damage. Overproduction of NO from the activation of iNOS during inflammation leads to the formation of O_2^-, contributing to the vicious cycle of oxidative stress and chronic inflammation associated with Chronic Kidney Disease (CKD). Guo *et al.* developed **A2**, a fluorescent probe enabling visualization of $ONOO^-$ flux in diabetic rat kidney tissue (Fig. 8(h)).[116] **A2** rapidly responded with turn-on fluorescence (within seconds) and boasted ultrahigh sensitivity (detection

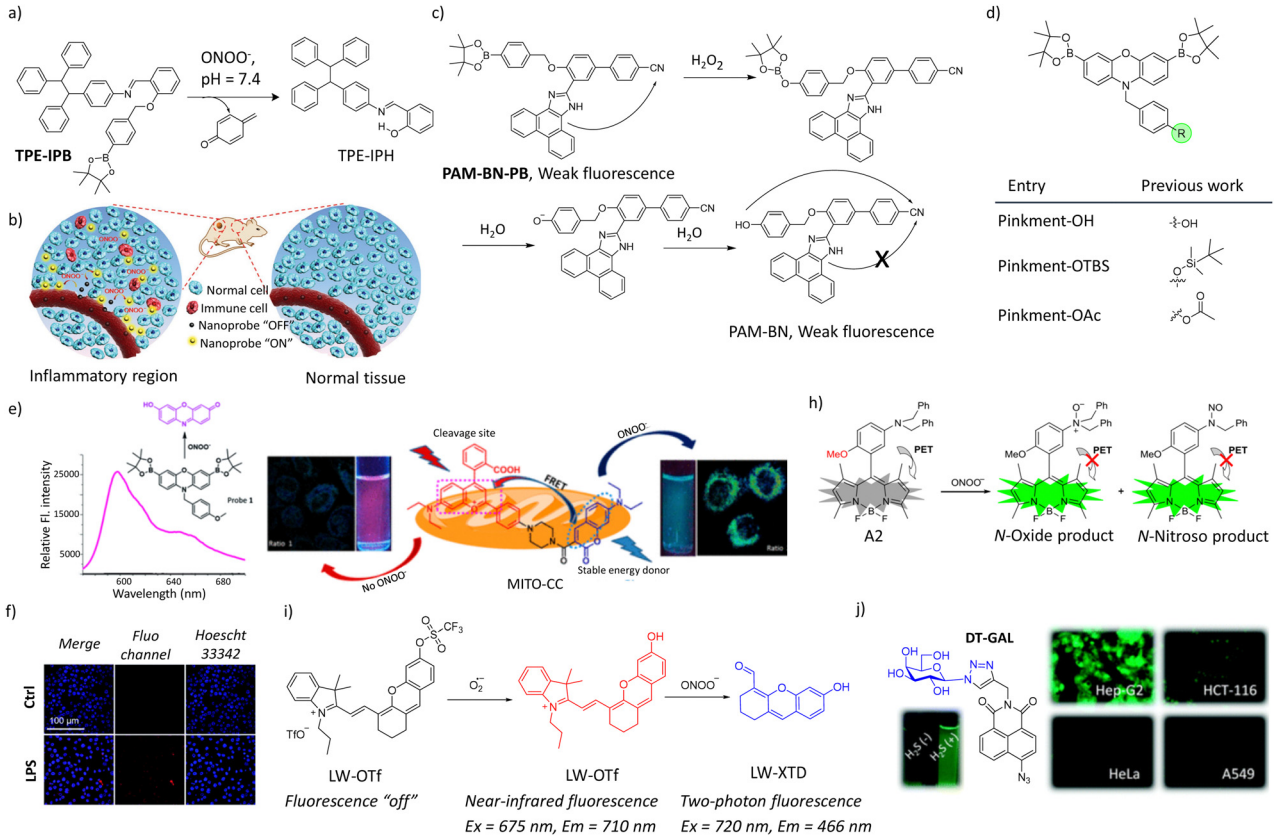

Fig. 8 Fluorescent probes for detecting RIS in inflammatory and liver, kidney and cardiovascular diseases. (a) Design of fluorescent nanoprobe **TPE–IPB–PEG** with AIE emission characteristics to accurately image $ONOO^-$ at the site of inflammation in bacterially infected mice (b). Reproduced with permission from ref. 111. Copyright 2016 Royal Society of Chemistry. (c) Design of **PAM–BN–PB** for the rapid imaging of H_2O_2 in mice afflicted with peritonitis. Reproduced with permission from ref. 112. Copyright 2017 American Chemical Society. (d) Design of **Pinkment**, a functionalized synthetic derivative of peroxyresorufin-1, for visualizing $ONOO^-$ in LPS-induced peritonitis mouse models. (e) Fluorescence spectra of Pinkment on interaction with $ONOO^-$. (f) Confocal imaging of RAW 264.7 macrophages treated with LPS (1 μg mL^{-1}, 24 h) and then loaded with Pinkment **8** (20 μM, 30 min). The cell nuclei were stained using Hoechst 33342. Scale bar = 100 μm. Reproduced with permission from ref. 114. Copyright 2020 Royal society of Chemistry. (g) Design of **MITO-CC**, a two-photon ratiometric fluorescence probe for the detection of $ONOO^-$ in cells and inflammation mouse models. Reproduced with permission from ref. 115. Copyright 2017 American Chemical Society. (h) Design of **A2**, a fluorescent probe enabling visualization of $ONOO^-$ flux in diabetic rat kidney tissue. Reproduced with permission from ref. 116. Copyright 2016 Elsevier. (i) Design of probe **LW-OTf** for detecting and imaging $O_2^{\bullet-}$ and $ONOO^-$ involved in drug involved liver injury (DILI). Reproduced with permission from ref. 117. Copyright 2021 Royal Society of Chemistry. (j) Design of **DT-Gal**, a galactosyl(azido) naphthalimide-based fluorogenic probe as a liver cell-specific probe for imaging H_2S in HepG2 liver cancer cells. Reproduced with permission from ref. 118. Copyright 2015 Royal Society of Chemistry.

limit: <2 nM), successfully visualizing endogenous $ONOO^-$ in RAW264.7 macrophages and oxygen-glucose-deprived endothelial cells and indicated elevated $ONOO^-$ concentration in diabetic kidney tissue (Fig. 8(h)). In chronic liver diseases, there is an elevation in oxidative stress which affects protein expression patterns. James *et al.* developed a molecular probe (**LW-OTf**) for detecting and imaging two biomarkers associated with drug-involved liver injury (DILI) (Fig. 8(i)). Initially, the ROS superoxide ($O_2^{\bullet-}$), selectively activates near-infrared fluorescence (NIRF) by generating the fluorophore LW-OH. This hemicyanine fluorophore is then oxidized by RNS peroxynitrite ($ONOO^-$), cleaving it to release the xanthene derivative LW-XTD, which is detected using two-photon excitation fluorescence (TPEF). Alternatively, LW-OTf can be cleaved by $ONOO^-$ to form non-fluorescent LW-XTD-OTf, which reacts with $O_2^{\bullet-}$ to produce the fluorescent LW-XTD. By combining NIRF and TPEF, LW-OTf enables the differential and simultaneous detection of ROS and RNS in DILI through two optically orthogonal channels.[117] Meanwhile, addressing the biological significance of H_2S, **DT-Gal**, a galactosyl(azido) naphthalimide-based fluorogenic probe, was developed (Fig. 8(j)).[118] Targeting liver cells with its galactosyl unit and reacting selectively with H_2S *via* its azido group, **DT-Gal** demonstrated its potential as a liver cell-specific probe for imaging H_2S in HepG2 liver cancer cells, offering insights into the role of abnormal H_2S levels in liver disease pathogenesis. Redox-sensitive factors such as Egr-1, NF-κB, AP-1, and kinases respond to these changes, driving cellular alterations and triggering hepatocyte apoptosis, which is a part of liver damage. The role of RSS in kidney and liver diseases remains unclear, as does the exact mechanism by which RONSS causes damage to these organs. All probes mentioned in this review have been summarized in Table 1.

Table 1 Summary of probes mentioned in this review

S. no	Name of molecule	Structure	RONSS detected	Disease	LOD	Ref.
1	CM2	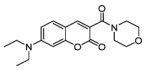	HOCl	AD	0.17 μM	8
2	QCy-BA	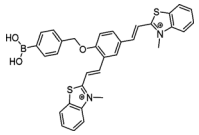	H_2O_2	Cancer	5.3 μM	9
3	3-HF-OMe	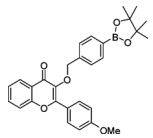	$ONOO^-$	AD	65.5 nM	51
4	BTNPO	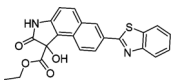	$ONOO^-$	AD	—	51
5	CRANAD 88	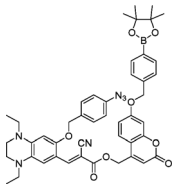	H_2O_2	AD	250 nM	52
6	DNPOCY	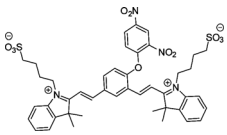	H_2S	AD	—	53
7	MITO-VS	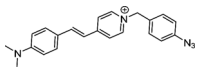	H_2S	AD	—	80
8	Mito NIRHV	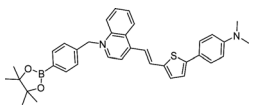	H_2O_2	AD	3 nM	81
9	BT-NH	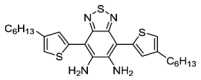	NO	PD	6.96 nM	82
10	NIR-PNs	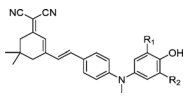	$ONOO^-$	PD	4.59 to 18.9 nM	83
11	TCAB	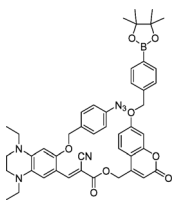	H_2S, H_2O_2	Cancer and other diseases	0.044 and 0.058 μM	86
12	HCY-ONO	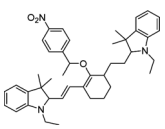	$O_2^{\bullet-}$, SO_2	Cancer, inflammation, cardiovascular disease	90 and 100 nM	87
13	BOD-NH-SC	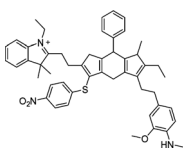	NO, H_2S	Various diseases	31 nM	88
14	TFP	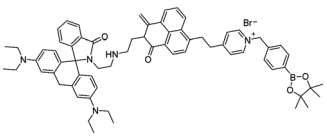	H_2O_2	Mitochondrial stress	0.4–10 μM	89

Table 1 (*continued*)

S. no	Name of molecule	Structure	RONSS detected	Disease	LOD	Ref.
15	MPIBA	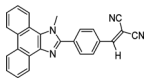	SO_2, ClO^-	Cancer	3.5 nM and 12.5 nM	102
16	TPE-IPB	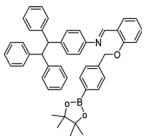	$ONOO^-$	Inflammation and other diseases	≈100 μM	111
17	PAM–BN–PB	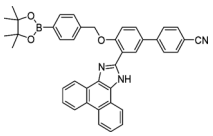	H_2O_2	Cancer, diabetes and neurodegeneration	148 nM	112
18	HOTN	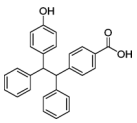	HOCl	Inflammation, cancer	0.108 μM	113
19	Pinkment probe	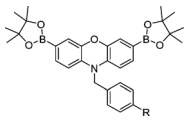	$ONOO^-$	Cancer	Not reported	114
20	MITO-CC	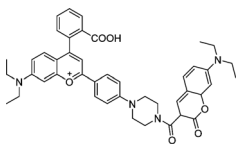	$ONOO^-$	Cancer and inflammation	11.30 nM	115
21	A2	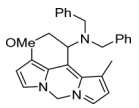	$ONOO^-$	Diabetes	2 nM	116
22	LW-OTf	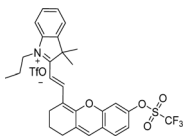	$O_2^{\bullet -}$, $ONOO^-$	Drug induced liver injury	46.5 nM and 38.2 nM	117
23	DT-GAL	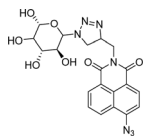	H_2S	Liver injury and cancer	0.78 μM	118

5. Conclusions and outlook

The father of medicine, Greek physician Hippocrates rightly said "Anything in excess is opposed to nature". Since their discovery more than a century ago, RONSS has long been viewed with the glasses of a critique, their role in physiology mostly being associated with detrimental effects and the progression of numerous diseases. Generation of RONSS is an intrinsic evolutionary trait, in the complex metabolic pathway of aerobic respiration and they play vital roles in the maintenance of optimum health, especially in cell signalling, transduction and immune response pathways. Excessive ROS production can however damage cellular components, including DNA, proteins, and lipids, leading to various chronic diseases such as cancer, neurodegenerative disorders, and cardiovascular diseases. Similarly, dysregulated production of RNS, can lead to the formation of toxic molecules like $ONOO^-$, contributing to tissue damage, mitochondrial dysfunction, and chronic inflammation, implicated in several pathological conditions, including atherosclerosis, sepsis, and autoimmune diseases. While RSS, especially H_2S contributes to cardiovascular health, neuroprotection, and anti-inflammatory responses, their dysregulation or excessive production can lead to tissue damage, and inflammation, and exacerbate disease conditions ranging from cancer to neurodegenerative diseases.

The precise detection of RONSS is critical for understanding their complex biological functions and contributions to disease progression. The development of improved probe sensitivity and specificity will enable real-time, *in vivo* monitoring of these species at the cellular and subcellular levels, offering insights into their roles in pathophysiology. Additionally, the integration of these

probes with imaging technologies and nanotechnology could lead to more precise diagnostics and targeted therapeutic interventions, potentially revolutionizing the management of oxidative stress-related disorders. Future advancements in RONSS therapeutics will rely on designing precise and selective molecular tools tailored to specific disease conditions. Probes for detecting RONSS must address disease-specific contexts. For example, in cancer, oxidative and nitrosative stress fluctuates within a heterogeneous tumor microenvironment influenced by hypoxia and overexpressed enzymes like nitroreductases. In contrast, neurodegenerative disorders involve chronic oxidative stress in neurons, necessitating probes with higher selectivity and long-term stability. Moreover, BBB permeability is a critical factor for targeting neurodegeneration, which is not essential for all cancer types. RONSS-targeting theranostics for cancer often integrate detection with therapeutic functions, such as ROS-triggered drug release. In contrast, neurodegeneration probes prioritize neuroprotection, incorporating antioxidants to mitigate oxidative damage while monitoring RONSS. While both aim to detect oxidative stress, their designs differ in addressing BBB permeability, species dynamics, target localization, and functional demands.

The future of therapeutics targeting RONSS lies in the development of more precise and selective agents that can modulate these reactive species to treat various diseases. Advances in antioxidant therapies will focus on fine-tuning redox balance rather than simply quenching these species, preserving their signaling roles while mitigating their harmful effects. Novel small molecules, gene therapies, and nanomedicine approaches could offer targeted delivery of these therapeutics, enhancing efficacy and reducing side effects. Additionally, the use of RSS-based therapies, such as H_2S donors, may emerge as promising treatments for conditions like neurodegenerative diseases, cardiovascular disorders, and cancer, where redox imbalance plays a critical role.

Despite massive research being directed towards the RONSS paradigm, their mechanism of action in many aspects of well-being and ailment remain poorly understood. Also, except for ROS and to an extent, RNS, the understanding of other species is still in infancy. Extensive research is required to lift the fog on how to arrive at the golden mean and deal best with this double-edged sword and tune the oxidant/antioxidant balance to maintain optimum health, longevity as well as fine-tune oxidative stress for therapeutic avenues.

Author contributions

TG conceptualized and supervised the manuscript, PB wrote the draft, DP wrote Section 3, HH wrote Section 4.1, MR wrote Section 4.4. Figures were made by PB with help from all other authors. All authors reviewed and edited the final draft of the review.

Conflicts of interest

There are no conflicts to declare.

Acknowledgements

The authors thank JNCASR, core grant (CRG/2020/004594), Science and Engineering Research Board (SERB), New Delhi, India, for the funding. DP, HH and MR thank DST India, CSIR and UGC for the student fellowships.

References

1 H. Sies, C. Berndt and D. P. Jones, *Annu. Rev. Biochem.*, 2017, **86**, 715–748.
2 H. Sies, in *Introductory Remarks* ed. H. B. T.-O. S. Sies, Academic Press, London, 1985, pp. 1–8.
3 S. Samanta, M. Ramesh and T. Govindaraju, *Alzheimer's Disease: Recent Findings in Pathophysiology, Diagnostic and Therapeutic Modalities*, The Royal Society of Chemistry, 2022, pp. 1–34.
4 J.-M. Noël and F. Kanoufi, *Curr. Opin. Electrochem.*, 2022, **35**, 101071.
5 J. Medrano-Macías, A. C. Flores-Gallegos, E. Nava-Reyna, I. Morales, G. Tortella, S. Solís-Gaona and A. Benavides-Mendoza, *Plants*, 2022, 11.
6 G. D. Puglia, *Plant Growth Regul.*, 2024, **103**, 9–32.
7 I. Pérez-Torres, M. E. Soto, V. Castrejón-Tellez, M. E. Rubio-Ruiz, L. Manzano Pech and V. Guarner-Lans, *Oxid. Med. Cell. Longevity*, 2020, **2020**, 8819719.
8 S. Samanta and T. Govindaraju, *ACS Chem. Neurosci.*, 2019, **10**, 4847–4853.
9 N. Narayanaswamy, S. Narra, R. R. Nair, D. K. Saini, P. Kondaiah and T. Govindaraju, *Chem. Sci.*, 2016, **7**, 2832–2841.
10 K. Rajasekhar, S. Samanta, V. Bagoband, N. A. Murugan and T. Govindaraju, *iScience*, 2020, **23**, 101005.
11 P. Baruah, H. Moorthy, M. Ramesh, D. Padhi and T. Govindaraju, *Chem. Sci.*, 2013, **14**, 9427–9438.
12 L. Wu, A. C. Sedgwick, X. Sun, S. D. Bull, X.-P. He and T. D. James, *Acc. Chem. Res.*, 2019, **52**, 2582–2597.
13 P. Gao, W. Pan, N. Li and B. Tang, *Chem. Sci.*, 2019, **10**, 6035–6071.
14 R. B. Ferreira, L. Fu, Y. Jung, J. Yang and K. S. Carroll, *Nat. Commun.*, 2022, **13**, 5522.
15 X. Peng and V. Gandhi, *Ther. Delivery*, 2012, **3**, 823–833.
16 X. Li, Y. Hu, X. Zhang, X. Shi, W. J. Parak and A. Pich, *Nat. Commun.*, 2024, **15**, 8172.
17 R. Das, J. Hardie, B. P. Joshi, X. Zhang, A. Gupta, D. C. Luther, S. Fedeli, M. E. Farkas and V. M. Rotello, *JACS Au*, 2022, **2**, 1679–1685.
18 D. A. Butterfield and B. Halliwell, *Nat. Rev. Neurosci.*, 2019, **20**, 148–160.
19 B. Commoner, J. Townsend and G. E. Pake, *Nature*, 1954, **174**, 689–691.
20 K. Chachlaki, J. Garthwaite and V. Prevot, *Nat. Rev. Endocrinol.*, 2017, **13**, 521–535.
21 G. I. Giles, M. J. Nasim, W. Ali and C. Jacob, *Antioxidants*, 2017, **6**, 38–42.
22 H. M. Smith and M. D. Pluth, *JACS Au*, 2023, **3**, 2677–2691.

23 O. M. Ighodaro and O. A. Akinloye, *Alexandria J. Med.*, 2018, **54**, 287–293.
24 P. R. Augusti, A. Quatrin, S. Somacal, G. M. Conterato, R. Sobieski, A. R. Ruviaro, L. H. Maurer, M. M. Duarte, M. Roehrs and T. Emanuelli, *J. Clin. Biochem. Nutr.*, 2012, **51**, 42–49.
25 H. Sies, V. V. Belousov, N. S. Chandel, M. J. Davies, D. P. Jones, G. E. Mann, M. P. Murphy, M. Yamamoto and C. Winterbourn, *Nat. Rev. Mol. Cell Biol.*, 2022, **23**, 499–515.
26 D. Garrido Ruiz, A. Sandoval-Perez, A. V. Rangarajan, E. L. Gunderson and M. P. Jacobson, *Biochemistry*, 2022, **61**, 2165–2176.
27 W. Zhang and H. T. Liu, *Cell Res.*, 2002, **12**, 9–18.
28 S. Alas, C. Ng and B. Bonavida, *Clinm Cancer Res.*, 2002, **8**, 836–845.
29 Z. Liu, M. Ma, D. Yu, J. Ren and X. Qu, *Chem. Sci.*, 2020, **11**, 11003–11008.
30 S. Li, Q. Zou, Y. Li, C. Yuan, R. Xing and X. Yan, *J. Am. Chem. Soc.*, 2018, **140**, 10794–10802.
31 A. L. D. Wallabregue, H. Bolland, S. Faulkner, E. M. Hammond and S. J. Conway, *J. Am. Chem. Soc.*, 2023, **145**, 2572–2583.
32 C. Yang, Q. Yang, Y. Xiang, X.-R. Zeng, J. Xiao and W.-D. Le, *Neural Regener. Res.*, 2023, **18**, 57–63.
33 H.-L. Zhou, R. Zhang, P. Anand, C. T. Stomberski, Z. Qian, A. Hausladen, L. Wang, E. P. Rhee, S. M. Parikh, S. A. Karumanchi and J. S. Stamler, *Nature*, 2019, **565**, 96–100.
34 G. Ferrer-Sueta and R. Radi, *ACS Chem. Biol.*, 2009, **4**, 161–177.
35 D. L. Miller and M. B. Roth, *Proc. Natl. Acad. Sci. U. S. A.*, 2007, **104**, 20618–20622.
36 B. D. Paul and S. H. Snyder, *Nat. Rev. Mol. Cell Biol.*, 2012, **13**, 499–507.
37 X. Ni, S. S. Kelly, S. Xu and M. Xian, *Acc. Chem. Res.*, 2021, **54**, 3968–3978.
38 J. Prousek, *Pure Appl. Chem.*, 2007, **79**, 2325–2338.
39 K. Rajasekhar and T. Govindaraju, *RSC Adv.*, 2018, **8**, 23780–23804.
40 S. J. Dixon, K. M. Lemberg, M. R. Lamprecht, R. Skouta, E. M. Zaitsev, C. E. Gleason, D. N. Patel, A. J. Bauer, A. M. Cantley, W. S. Yang, B. Morrison 3rd and B. R. Stockwell, *Cell*, 2012, **149**, 1060–1072.
41 P. Maher, A. Currais and D. Schubert, *Cell Chem. Biol.*, 2020, **27**, 1456–1471.
42 P. Tsvetkov, S. Coy, B. Petrova, M. Dreishpoon, A. Verma, M. Abdusamad, J. Rossen, L. Joesch-Cohen, R. Humeidi, R. D. Spangler, J. K. Eaton, E. Frenkel, M. Kocak, S. M. Corsello, S. Lutsenko, N. Kanarek, S. Santagata and T. R. Golub, *Science*, 2022, **375**, 1254–1261.
43 S. Samanta, K. Rajasekhar, M. Ramesh, N. A. Murugan, S. Alam, D. Shah, J. P. Clement and T. Govindaraju, *Adv. Ther.*, 2021, **4**, 2000225.
44 M. Ramesh and T. Govindaraju, *Chem. Sci.*, 2022, **13**, 13657–13689.
45 H. Arora, M. Ramesh, K. Rajasekhar and T. Govindaraju, *Bull. Chem. Soc. Jpn.*, 2020, **93**, 507–546.
46 K. Rajasekhar, M. Chakrabarti and T. Govindaraju, *Chem. Commun.*, 2015, **51**, 13434–13450.
47 K. Rajasekhar, K. Mehta and T. Govindaraju, *ACS Chem. Neurosci.*, 2018, **9**, 1432–1440.
48 T. Ueno and T. Nagano, *Nat. Methods*, 2011, **8**, 642–645.
49 Y. Geng, Z. Wang, J. Zhou, M. Zhu, J. Liu and T. D. James, *Chem. Soc. Rev.*, 2023, **52**, 3873–3926.
50 J. Ke, P. Zhao, J. Li and Q. Fu, *J. Mater. Chem. B*, 2022, **10**, 8744–8749.
51 A. C. Sedgwick, W.-T. Dou, J.-B. Jiao, L. Wu, G. T. Williams, A. T. A. Jenkins, S. D. Bull, J. L. Sessler, X.-P. He and T. D. James, *J. Am. Chem. Soc.*, 2018, **140**, 14267–14271.
52 J. Yang, J. Yang, S. H. Liang, Y. Xu, A. Moore and C. Ran, *Sci. Rep.*, 2016, **6**, 35613.
53 D. Maity, A. Raj, P. K. Samanta, D. Karthigeyan, T. K. Kundu, S. K. Pati and T. Govindaraju, *RSC Adv.*, 2014, **4**, 11147–11151.
54 S. Ghatak, T. Nakamura and S. A. Lipton, *Front. Neural Circuits*, 2023, **17**, 1099467.
55 P. Wang, L. Yu, J. Gong, J. Xiong, S. Zi, H. Xie, F. Zhang, Z. Mao, Z. Liu and J. S. Kim, *Angew. Chem., Int. Ed.*, 2022, **61**, e202206894.
56 E. Disbrow, K. Y. Stokes, C. Ledbetter, J. Patterson, R. Kelley, S. Pardue, T. Reekes, L. Larmeu, V. Batra, S. Yuan, U. Cvek, M. Trutschl, P. Kilgore, J. S. Alexander and C. G. Kevil, *Alzheimer's Dementia*, 2021, **17**, 1391–1402.
57 K. Rajasekhar, C. Madhu and T. Govindaraju, *ACS Chem. Neurosci.*, 2016, **7**, 1300–1310.
58 K. Rajasekhar, N. Narayanaswamy, N. A. Murugan, G. Kuang, H. Ågren and T. Govindaraju, *Sci. Rep.*, 2016, **6**, 23668.
59 S. Mandal, Y. V. Suseela, S. Samanta, B. Vileno, P. Faller and T. Govindaraju, *ACS Med. Chem. Lett.*, 2024, **15**, 1376–1385.
60 S. Samanta, K. Rajasekhar, V. Babagond and T. Govindaraju, *ACS Chem. Neurosci.*, 2019, **10**, 3611–3621.
61 S. Park, M. Kim, Y. Lin, M. Hong, G. Nam, A. Mieczkowski, J. Kardos, Y.-H. Lee and M. H. Lim, *Chem. Sci.*, 2023, **14**, 9293–9305.
62 M. Ramesh, C. Balachandra, P. Andhare and T. Govindaraju, *ACS Chem. Neurosci.*, 2022, **13**, 2209–2221.
63 D. Padhi, C. Balachandra, M. Ramesh and T. Govindaraju, *Chem. Commun.*, 2022, **58**, 6288–6291.
64 D. Padhi, P. Baruah, M. Ramesh, H. Moorthy and T. Govindaraju, *Redox Biol.*, 2024, **71**, 103119.
65 J. Wang, P. Shangguan, X. Chen, Y. Zhong, M. Lin, M. He, Y. Liu, Y. Zhou, X. Pang, L. Han, M. Lu, X. Wang, Y. Liu, H. Yang, J. Chen, C. Song, J. Zhang, X. Wang, B. Shi and B. Z. Tang, *Nat. Commun.*, 2024, **15**, 705.
66 R. Alvariño, E. Alonso, M. E. Abbasov, C. M. Chaheine, M. L. Conner, D. Romo, A. Alfonso and L. M. Botana, *ACS Chem. Neurosci.*, 2019, **10**, 4102–4111.
67 M. Dodson, R. Castro-Portuguez and D. D. Zhang, *Redox Biol.*, 2019, **23**, 101107.

68 M.-C. Lu, J. Zhao, Y.-T. Liu, T. Liu, M.-M. Tao, Q.-D. You and Z.-Y. Jiang, *Redox Biol.*, 2019, **26**, 101266.
69 H. Moorthy, L. P. Datta, S. Samanta and T. Govindaraju, *ACS Appl. Mater. Interfaces*, 2022, **14**, 56535–56547.
70 H. Moorthy, M. Ramesh, D. Padhi, P. Baruah and T. Govindaraju, *Mater. Horiz.*, 2024, **11**, 3082–3089.
71 Y. Liu, Y. Chen, Y. Gong, H. Yang and J. Liu, *ACS Appl. Nano Mater.*, 2023, **6**, 5384–5393.
72 Y. Wang, Y. Huang, A. Ma, J. You, J. Miao and J. Li, *J. Agric. Food Chem.*, 2024, **72**, 11854–11870.
73 X. Wu, X. Sun, Z. Guo, J. Tang, Y. Shen, T. D. James, H. Tian and W. Zhu, *J. Am. Chem. Soc.*, 2014, **136**, 3579–3588.
74 M. Iciek, A. Bilska-Wilkosz, M. Kozdrowicki and M. Górny, *Biosci. Rep.*, 2022, **42**, BSR20221006.
75 Y. V. Suseela, P. Satha, N. A. Murugan and T. Govindaraju, *Theranostics*, 2020, **10**, 10394–10414.
76 C. Hao, A. Qu, L. Xu, M. Sun, H. Zhang, C. Xu and H. Kuang, *J. Am. Chem. Soc.*, 2019, **141**, 1091–1099.
77 R. N. Kalaria, G. E. Maestre, R. Arizaga, R. P. Friedland, D. Galasko, K. Hall, J. A. Luchsinger, A. Ogunniyi, E. K. Perry, F. Potocnik, M. Prince, R. Stewart, A. Wimo, Z. X. Zhang and P. Antuono, *Lancet Neurol.*, 2008, **7**, 812–826.
78 G. Cenini, A. Lloret and R. Cascella, *Oxid. Med. Cell. Longevity*, 2019, **2019**, 2105607.
79 E. O. Olufunmilayo, M. B. Gerke-Duncan and R. M. D. Holsinger, *Antioxidants*, 2023, **12**, 517.
80 S.-J. Li, Y.-F. Li, H.-W. Liu, D.-Y. Zhou, W.-L. Jiang, J. Ou-Yang and C.-Y. Li, *Anal. Chem.*, 2018, **90**, 9418–9425.
81 S. Li, P. Wang, W. Feng, Y. Xiang, K. Dou and Z. Liu, *Chem. Commun.*, 2020, **56**, 1050–1053.
82 M. Weng, X. Yang, Y. Ni, C. Xu, H. Zhang, J. Shao, N. Shi, C. Zhang, Q. Wu, L. Li and W. Huang, *Sens. Actuators, B*, 2019, **283**, 769–775.
83 Q. Sun, J. Xu, C. Ji, M. S. S. Shaibani, Z. Li, K. Lim, C. Zhang, L. Li and Z. Liu, *Anal. Chem.*, 2020, **92**, 4038–4045.
84 Y.-Q. Yuan, Y.-L. Wang, B.-S. Yuan, X. Yuan, X.-O. Hou, J.-S. Bian, C.-F. Liu and L.-F. Hu, *Brain, Behav., Immun.*, 2018, **67**, 77–90.
85 A. Gaspar, M. J. Matos, J. Garrido, E. Uriarte and F. Borges, *Chem. Rev.*, 2014, **114**, 4960–4992.
86 L. Yang, Y. Zhang, X. Ren, B. Wang, Z. Yang, X. Song and W. Wang, *Anal. Chem.*, 2020, **92**, 4387–4394.
87 M. Gao, X. Zhang, Y. Wang, Q. Liu, F. Yu, Y. Huang, C. Ding and L. Chen, *Anal. Chem.*, 2019, **91**, 7774–7781.
88 T. Zhu, N. Ren, X. Liu, Y. Dong, R. Wang, J. Gao, J. Sun, Y. Zhu, L. Wang, C. Fan, H. Tian, J. Li and C. Zhao, *Angew. Chem., Int. Ed.*, 2021, **60**, 8450–8454.
89 Z. Wu, M. Liu, Z. Liu and Y. Tian, *J. Am. Chem. Soc.*, 2020, **142**, 7532–7541.
90 S. Fahn, *Ann. Neurol.*, 1992, **32**, S128–S132.
91 C. W. Shults, D. Oakes, K. Kieburtz, M. F. Beal, R. Haas, S. Plumb, J. L. Juncos, J. Nutt, I. Shoulson, J. Carter, K. Kompoliti, J. S. Perlmutter, S. Reich, M. Stern, R. L. Watts, R. Kurlan, E. Molho, M. Harrison, M. Lew and Parkinson Study Group, *Arch. Neurol.*, 2002, **59**, 1541–1550.
92 D. T. Dexter, S. A. Statton, C. Whitmore, W. Freinbichler, P. Weinberger, K. F. Tipton, L. Della Corte, R. J. Ward and R. R. Crichton, *J. Neural Transm.*, 2011, **118**, 223–231.
93 L.-Y. Su, H. Li, L. Lv, Y.-M. Feng, G.-D. Li, R. Luo, H.-J. Zhou, X.-G. Lei, L. Ma, J.-L. Li, L. Xu, X.-T. Hu and Y.-G. Yao, *Autophagy*, 2015, **11**, 1745–1759.
94 P. E. Chabrier and M. Auguet, *CNS Drug Rev.*, 2007, **13**, 317–332.
95 Z. Xun, S. Rivera-Sánchez, S. Ayala-Peña, J. Lim, H. Budworth, E. M. Skoda, P. D. Robbins, L. J. Niedernhofer, P. Wipf and C. T. McMurray, *Cell Rep.*, 2012, **2**, 1137–1142.
96 S. Han, J.-R. Choi, K. Soon Shin and S. J. Kang, *Brain Res.*, 2012, **1483**, 112–117.
97 K. Tanaka, T. Kanno, Y. Yanagisawa, K. Yasutake, S. Inoue, N. Hirayama and J.-E. Ikeda, *PLoS One*, 2014, **9**, e87728.
98 I. I. C. Chio and D. A. Tuveson, *Trends Mol. Med.*, 2017, **23**, 411–429.
99 Y. Huo, P. Selenica, A. H. Mahdi, F. Pareja, K. Kyker-Snowman, Y. Chen, R. Kumar, A. Da Cruz Paula, T. Basili, D. N. Brown, X. Pei, N. Riaz, Y. Tan, Y.-X. Huang, T. Li, N. J. Barnard, J. S. Reis-Filho, B. Weigelt and B. Xia, *npj Breast Cancer*, 2021, **7**, 45.
100 S. S. Sabharwal and P. T. Schumacker, *Nat. Rev. Cancer*, 2014, **14**, 709–721.
101 E. L. Mills, D. G. Ryan, H. A. Prag, D. Dikovskaya, D. Menon, Z. Zaslona, M. P. Jedrychowski, A. S. H. Costa, M. Higgins, E. Hams, J. Szpyt, M. C. Runtsch, M. S. King, J. F. McGouran, R. Fischer, B. M. Kessler, A. F. McGettrick, M. M. Hughes, R. G. Carroll, L. M. Booty, E. V. Knatko, P. J. Meakin, M. L. J. Ashford, L. K. Modis, G. Brunori, D. C. Sévin, P. G. Fallon, S. T. Caldwell, E. R. S. Kunji, E. T. Chouchani, C. Frezza, A. T. Dinkova-Kostova, R. C. Hartley, M. P. Murphy and L. A. O'Neill, *Nature*, 2018, **556**, 113–117.
102 K. Dou, Q. Fu, G. Chen, F. Yu, Y. Liu, Z. Cao, G. Li, X. Zhao, L. Xia, L. Chen, H. Wang and J. You, *Biomaterials*, 2017, **133**, 82–93.
103 M. Wang, M. Chang, C. Li, Q. Chen, Z. Hou, B. Xing and J. Lin, *Adv. Mater.*, 2022, **34**, 2106010.
104 W. Zhang, X. Hu, Q. Shen and D. Xing, *Nat. Commun.*, 2019, **10**, 1704.
105 I. Okamoto, H. Miyaji, S. Miyata, K. Shitomi, T. Sugaya, N. Ushijima, T. Akasaka, S. Enya, S. Saita and H. Kawasaki, *ACS Omega*, 2021, **6**, 9279–9290.
106 A. M. Fleming, Y. Ding and C. J. Burrows, *Proc. Natl. Acad. Sci. U. S. A.*, 2017, **114**, 2604–2609.
107 S. Cogoi, A. Ferino, G. Miglietta, E. B. Pedersen and L. E. Xodo, *Nucleic Acids Res.*, 2018, **46**, 661–676.
108 Y. Venkata Suseela, P. Sengupta, T. Roychowdhury, S. Panda, S. Talukdar, S. Chattopadhyay, S. Chatterjee and T. Govindaraju, *ACS Bio Med Chem Au*, 2022, **2**, 125–139.
109 K. Lingappan, *Curr. Opin. Toxicol.*, 2018, **7**, 81–86.
110 A. Mongirdienė, L. Skrodenis, L. Varoneckaitė, G. Mierkytė and J. Gerulis, *Biomedicines*, 2022, **10**, 602–607.
111 Z. Song, D. Mao, S. H. P. Sung, R. T. K. Kwok, J. W. Y. Lam, D. Kong, D. Ding and B. Z. Tang, *Adv. Mater.*, 2016, **28**, 7249–7256.

112 Y. Chen, X. Shi, Z. Lu, X. Wang and Z. Wang, *Anal. Chem.*, 2017, **89**, 5278–5284.
113 X. Han, Y. Ma, Y. Chen, X. Wang and Z. Wang, *Anal. Chem.*, 2020, **92**, 2830–2838.
114 M. Weber, H.-H. Han, B.-H. Li, M. L. Odyniec, C. E. F. Jarman, Y. Zang, S. D. Bull, A. B. Mackenzie, A. C. Sedgwick, J. Li, X.-P. He and T. D. James, *Chem. Sci.*, 2020, **11**, 8567–8571.
115 D. Cheng, Y. Pan, L. Wang, Z. Zeng, L. Yuan, X. Zhang and Y.-T. Chang, *J. Am. Chem. Soc.*, 2017, **139**, 285–292.
116 J. Miao, Y. Huo, Q. Liu, Z. Li, H. Shi, Y. Shi and W. Guo, *Biomaterials*, 2016, **107**, 33–43.
117 L. Wu, J. Liu, X. Tian, R. R. Groleau, S. D. Bull, P. Li, B. Tang and T. D. James, *Chem. Sci.*, 2021, **12**, 3921–3928.
118 D.-T. Shi, D. Zhou, Y. Zang, J. Li, G.-R. Chen, T. D. James, X.-P. He and H. Tian, *Chem. Commun.*, 2015, **51**, 3653–3655.
119 P. Pacher, J. S. Beckman and L. Liaudet, *Physiol. Rev.*, 2007, **87**, 315–424.
120 M. V. Irazabal and V. E. Torres, *Cells*, 2020, **9**, 1342.